DGR 1800 del 15 dicembre 2021

2° PERIODO DI PROGETTO –RELAZIONE FINALE PROGETTO INERTEX

WP-3

TITOLO DELIVERABLE

D11_bis - Report contenente i risultati della sperimentazione relativa alla inertizzazione e stabilizzazione di suoli inquinati.

CONTENUTI

1. Obiettivi iniziali
2. Metodologia adottata
3. Risultati ottenuti
4. Ruoli e attività svolta dai partner
5. Ruoli e attività svolta dai consulenti
6. Documentazione fotografica, schemi

1. Obiettivi iniziali

L'obiettivo è stato sperimentare un processo di stabilizzazione di terreni contaminati da piombo con leganti tradizionali e alternativi.
La contaminazione del suolo dovuta alla presenza di metalli pesanti è efficientemente trattata con tecnologie basate sull'immobilizzazione come la solidificazione/stabilizzazione (S/S); il processo comprende sia l'immobilizzazione chimica dei contaminanti che la stabilizzazione fisica del suolo facendo reagire i contaminanti matrice con un legante idraulico (tipicamente Cemento Portland Ordinario, OPC).
Nonostante la chimica dell'OPC come materiale da costruzione sia conosciuta, i meccanismi che controllano l'immobilizzazione dei metalli pesanti nei sistemi cemento-terreno non sono così conosciuti.
Secondo la teoria, l'S/S con il cemento provoca la precipitazione o coprecipitazione degli ioni metallici come idrossidi o nei loro assorbimenti da parte dei prodotti di idratazione del cemento, ad esempio nel silicato di calcio idrato, o fasi di tipo ettringite e/o monosolfato.
Tuttavia, i tentativi sperimentali di dimostrare questa teoria non forniscono prove dirette ex post complete ma, nella maggior parte dei casi, si riferiscono ad ex-ante sintesi e caratterizzazione dei materiali preparati.
La formazione occasionale di nuove fasi mineralogiche contenenti cationi metallici tossici o ossianioni sono state segnalate, ma il ruolo di queste fasi nella ritenzione degli elementi tossici non è sempre evidente e chiara.
Molti studi sono stati poi pubblicati riguardanti l'idratazione dei metalli drogati OPC o fasi singole di cemento, ma sebbene altamente informativi nel valutare l'effetto di diversi elementi pericolosi sulle reazioni di idratazione e sulle proprietà di lisciviazione, non sono rappresentativi delle reali condizioni di contaminazione.

Nella realizzazione degli obiettivi, OPIGEO ha coordinato il lavoro e i partner di progetto hanno svolto attività di supporto: le attività direttamente sono descritte successivamente.

Come previsto dal progetto, OPIGEO ha inoltre affidato all'Università di Padova, Centro interdipartimentale CIRCE, la realizzazione di uno studio specifico di approfondimento per valutare ipotesi di lavoro particolarmente innovative e da sperimentare nel corso del progetto. Nel secondo periodo non sono stato necessarie ulteriori attività da parte di CIRCE avendo conseguito gli obiettivi specifici già nel primo periodo. I risultati di questo studio sono contenuti in un articolo scientifico denominato "*Stabilization of lead contaminated soil with traditional and alternative binders*", che costituisce la Relazione Tecnica di CIRCE, presente in allegato (l'articolo era già stato inviato con la Relazione Intermedia, per comodità di lettura si ripropone) e a cui si rimanda per dettagli, evitando di riscrivere contenuti identici.

2. Metodologia

Nel secondo periodo sono stati eseguite valutazioni relative alla stabilizzazione dei terreni mediante l'impiego di aggregati destinati al trattamento acque contaminate. Lo scopo riguarda la valutazione delle prestazioni meccaniche ed adsorbenti nell'impiego combinato di leganti idraulici alternativi e aggregati porosi destinati al trattamento acque.

Per simulare l'applicazione in ambito geotecnico è stato realizzato un dimostratore basato su un sistema di filtrazione configurato con l'impiego di n°4 cisterne da 1000 litri per contenimento di acqua contaminata e acqua filtrata, n 6 fusti in PE da 60 litri collegati in serie per contenimento del mix granulato filtrante, legante idraulico alternativo e terreno, un sistema di pompe e raccorderia idraulica atto a garantire il flusso di acqua in ingresso e in uscita.

E’ stato simulato un passaggio del fluido contaminato, dalle cisterne attraverso il mix di granulato filtrante, legante idraulico alternativo e terreno, al fine di valutare le proprietà adsorbenti del composito filtrante e le proprietà meccaniche del terreno in seguito a progressiva fisiologica compattazione del composito stesso.

Sono stati impiegati mezzi d’opera per movimento terra (n°1 scavatore da 37 q.li; n° 1 scavatore da 60 q.li; n° 1 trattore con fresa a martelli) per la messa in opera del materiale inertizzato su un percorso sterrato al servizio di un cantiere, compattarlo e valutarne il comportamento sotto sollecitazione meccanica.

Riepilogando, i lavori sono stati portati avanti in due direzioni:

- uno studio condotto da CIRCE sull'applicazione di un innovativo processo di solidificazione/stabilizzazione (S/S) per la bonifica di terreni contaminati da Pb;
- uno studio sulla selezione e definizione delle procedure e tecnologie di lavorazione delle miscele minerali nella inertizzazione dei terreni contaminati.

In relazione al primo punto, l’articolo citato nel paragrafo precedente dettaglio il tutto.
In relazione al secondo punto sono state selezionate le procedure che di seguito sono descritte.
Le responsabilità relative alla gestione del processo di trattamento sono così suddivise:

- Verifica preliminare della documentazione: Responsabile Bonifiche
- Gestione e verifica dei formulari di trasporto rifiuto - Gestione registri di carico e scarico: Responsabile gestione rifiuti

Procedure di lavorazione
La tecnologia di trattamento viene applicata secondo le seguenti fasi distinte:

1. Scavo dei rifiuti da trattare
2. Fase di preparazione
3. Fase di miscelazione
4. Fase di granulazione
5. Fase di maturazione

Il processo di inertizzazione (solidificazione/stabilizzazione) si basa sull’azione stabilizzante dei processi di idratazione del cemento, dove alcuni metalli co-precipitano con idrossidi di calcio ed in ogni caso vengono immobilizzati dal reticolo cementizio.
L’azione anticomplessante è a carico di additivi (es.: quelli verificati Mapei), che inibisce la formazione di complessimetallici (es. ammoniacali) che non precipiterebbero e favorisce la precipitazione di metalli come solfuri poi conglobati nel cemento. L’azione superfluidificante e idrofobizzante di un secondo additivo, consente di ridurre la quantità di acqua da aggiungere al processo, riducendo anche la porosità del materiale finale. Al termine del trattamento il rifiuto si presenta sottoforma di granulidi conglomerato cementizio di dimensioni limitate (max 2 – 3 cm) e caratterizzati da cessioni nulle (o estremamente ridotte), elevate proprietà meccaniche e di durabilità.

Il processo non prevede la produzione di emissioni in atmosfera dal momento che esegue, sostanzialmente, una attività di miscelazione ad umido del rifiuto con leganti idraulici, additivi ed acqua ed un successivo processo di granulazione (anch’esso con aggiunta di acqua su un impasto umido). Le prove di trattamento sperimentale non produrranno in egual misura scarichi idrici, in quanto le acque di processo (utilizzate per il condizionamento ad umido), una volta completato il trattamento, saranno aspirate e inviate a trattamento in impianti autorizzati off-site.

Scavo dei rifiuti da trattare e caratterizzazione preventiva
Il rifiuto da trattare viene escavato presso l'areale del sito di prova in posizioni individuate. Prelevato mediante escavatore a mezzo di trincea esplorativa (profondità massima pari a circa 1-1,5 m da p.c.) e disposto in cumulo sulla platea dell'impianto, per la successiva fase di trattamento.
A seguito dello scavo si procede alle analisi chimiche di caratterizzazione del rifiuto prima del trattamento. La caratterizzazione preventiva del rifiuto ha lo scopo di evidenziare le fasi presenti e l'eterogeneità dei materiali. La caratterizzazione riguarda i seguenti livelli di conoscenza:

- **Mineralogica**, mediante diffrazione ai raggi X da polveri (XRPD),
- **Chimica**, mediante fluorescenza a raggi X (XRF),
- **Spettroscopica**, mediante spettroscopia infrarossa (FTIR) e micro-Raman.

Sul materiale derivante dagli scavi e depositato in cumulo presso l'apposita platea si eseguono analisi sia sul tal quale sia mediante test di cessione (DM 5/2/98).
Le analisi sono eseguite sui seguenti parametri.

PARAMETRI FISICI	SOSTANZE ORGANICHE
Aspetto fisico	Carbonio organico totale (TOC)
Residuo a 105 °C	Solventi organici aromatici
Residuo a 600 °C	Solventi organici clorurati
pH	Solventi organici volatili
METALLI PESANTI	Policlorobifenili totali (PCB)
Arsenico (As)	Speciazione classi idrocarburiche
Antimonio (Sb)	Idrocarburi leggeri (C<12)
Cadmio (Cd)	Idrocarburi pesanti (C>12)
Cromo (Cr)	Idrocarburi Policiclici Aromatici (IPA)

I risultati che fanno fede nella definizione dei rifiuti che dovranno essere sottoposti a trattamento sono quelli a mezzo di test di cessione: il trattamento sperimentale verrà eseguito se saranno rilevatii contaminanti sopra indicati in concentrazioni maggiori a quelle previste in Allegato 3 al DM 5/2/98.Le analisi sul tal quale avranno solo carattere conoscitivo.
Le analisi vengono eseguite in ragione di 1 per ogni cumulo da sottoporre a trattamento (R1, R2,R3).

Fase di preparazione al trattamento
A seguito dello scavo delle trincee e successivo stoccaggio nelle aree di deposito dedicate, l'iter di trattamento del rifiuto prevede:

- Maturazione iniziale per disidratazione gravitativa in cumulo coperto (umidità ideale inferiore al 30%).
- Vagliatura con vibrovaglio con passo da 4 mm, al fine di ottenere in ingresso al miscelatore un materiale con granulometria <4 mm.
- Verifica della possibilità di recupero del sopravaglio o macinazione per riduzione a <4mm (la fase di macinazione non è prevista nell'ambito delle prove sperimentali in questione; inoltre, a recepimento di quanto emerso in fase di Screening VIA, il materiale di sopravaglio prodotto nel corso della prova di trattabilità verrà inviato a recupero/smaltimento presso impianti autorizzati off-site).

Fase di miscelazione e trattamento
Sulla base dei risultati delle analisi chimiche di caratterizzazione preliminare del rifiuto, vi è il passaggio alla formulazione di "ricette" specifiche per le prove di trattamento e all'applicazione delle diverse ricette ed esecuzione delle prove di trattamento. Nella ricetta vengono registrati i variparametri del campione. Segue dunque la Fase di miscelazione, con inserimento del rifiuto in un miscelatore intensivo a vomeri con l'aggiunta del legante individuato, degli additivi ed eventualmente di un'aliquota di acqua,per ottenere un impasto arido.

Fase di granulazione
La fase di granulazione avviene con passaggio del materiale in un piatto rotante ad asse inclinato, dove si formano i granuli. Anche in questa fase viene aggiunta un'ulteriore aliquota di acqua per ottenere la granulazione alla dimensione desiderata (l'optimum ai fini del riutilizzo è un fuso granulometrico da 8 a 20 mm), regolabile sia con la quantità d'acqua che con il tempo di permanenzanel piatto granulatore attraverso la sua inclinazione.

Test sui parametri di processo intermedi
A seguito della maturazione a secco, verranno eseguite sul materiale analisi sia sul tal quale sia mediante test di cessione (DM 5/2/98) sui parametri indicati in tabella 3.
I risultati verranno confrontati con l'Allegato 3 del DM 5/2/98 e con la tabella 2 dell'Allegato 5 al Titolo V della parte quarta del D. Lgs.152/06.

Fase di maturazione
Al fine di ottimizzare il reticolo cristallino all'interno del granulato, si prevede la seguente fase di maturazione:

- I pellet scaricati vengono stesi in strati da 0,5 m, per un primo indurimento.
- I pellet induriti vengono trasferiti in cumulo per la maturazione.
- Dopo all'incirca 20 giorni la maturazione può prevedere una fase di condizionamento ad umido. Tale fase avviene immergendo i granuli in vasche piene d'acqua in cui viene insufflata aria compressa. Lo scopo di questa fase è duplice:
  i) attraverso la carbonatazione della calce idrata e delle fasi cementizie idratate che costituiscono i granuli, il pH scende al di sotto del valore limite previsto per il riutilizzo (pH = 12);
  ii) vengono fissati alcuni metalli aventi caratteristiche anfotere.

La durata del trattamento di condizionamento ad umido varia a seconda dei casi, in funzionedel tipo di rifiuto da trattare e della ricetta applicata, ma comunque non è inferiore a 20 giorni.

Verifica delle caratteristiche
Conclusa la fase di maturazione, i materiali trattati vengono sottoposti alle analisi chimiche di verificadelle caratteristiche ambientali e geotecniche dei materiali trattati.
Le analisi post-trattamento verranno eseguite sui granuli prodotti e sottoposti sia a sola maturazionea secco sia a maturazione associata a condizionamento ad umido.
Su ogni partita di granuli ottenuti mediante le diverse ricette di trattamento testate saranno eseguitele analisi di cui al paragrafo precedente (in particolare analisi XRPD, XRF, SEM-EDS, FTIR, Raman) al fine di definire il rapporto rifiuto/binder, tipo di binder e tipo di additivo. Oltre a quanto appena indicato si analizzerà la porosità dei granuli, ed eventualmente verranno effettuate ulteriori misure mirate a comprendere in dettaglio i meccanismi di stabilizzazione. Tali attività analitiche sono finalizzate alla comprensione dei meccanismi e delle reazioni che controllano l'immobilizzazione degli inquinanti nel

sistema cemento-rifiuto, ad esplorare il meccanismo di solidificazione durantel'idratazione del binder, ed analizzare in dettaglio la distribuzione degli inquinanti ed i meccanismi diimmobilizzazione degli stessi.

In particolare, sul rifiuto trattato vengono eseguite le seguenti prove:

- Indice di appiattimento (frazione > 4 mm) secondo UNI EN 933/3
- Indice di forma (frazione > 4 mm) secondo UNI EN 933/4
- Resistenza alla frammentazione (Los Angeles) secondo UNI EN 1097-6:2002
- Resistenza all'abrasione (Micro-Deval) secondo UNI EN 1097-6:2002
- Contenuto di solfati solubili in acido secondo UNI EN 1744-1:1999
- Contenuto di cloruri solubili in acqua secondo UNI EN 1744-1:1999
- Determinazione dell'influenza di un estratto di aggregato sul tempo di inizio presa delcemento secondo UNI EN 1744-6:2007
- Distribuzione granulometrica e modulo di finezza secondo UNI EN 933-1:1999
- Indice di appiattimento secondo UNI EN 933-3:2004
- Equivalente in sabbia secondo UNI EN 933-8:2000
- Indice di forma secondo UNI EN 933-4:2002
- Dimensione massima Dmax secondo UNI EN 933-1:1999

Per quanto riguarda i limiti di accettabilità, farà riferimento quanto previsto per gli aggregati da riciclo per le diverse applicazioni negli allegati C1, C2, C3, C4, C5 alla Circolare Ministeriale n. 5205del 15/07/2005 "Indicazioni per l'operatività nel settore edile, stradale e ambientale, ai sensi del decreto ministeriale 8 maggio 2003, n. 203", al D.P.R. 21/04/1993, n.246 e al Decreto Ministeriale9 marzo 1988 n.126 e ss.mm.
Le prove verranno eseguite sui campioni che avranno superato positivamente la fase di verifica aglistandard ambientali già precedentemente specificati.
Analogamente a quanto previsto per la fase di precaratterizzazione del rifiuto, anche sui granuli prodotti si procederà ad eseguire l'analisi mediante test di cessione ai sensi del DM 5/2/98 e s.m.i.,applicando il set analitico ed i limiti di riferimento. A conclusione dei controlli verrà compilata la Dichiarazione di conformità finale del rifiuto trattato.

Definizione ed etichettatura dei lotti di produzione
Il lotto viene definito in partenza in base all'area di scavo. A seguito della granulazione e della maturazione una parte del materiale verrà opportunamente raccolto e conferito presso la sede per effettuare analisi successive. La massa del lotto non deve superare i 100 kg.
Il lotto verrà opportunamente indicato tramite etichettatura come da modello predisposto. Anche le aree di stoccaggio verranno opportunamente contraddistinte da specifiche etichette.

Prove di lungo periodo
Nel secondo periodo sono stati effettuate le analisi su un campione di granulato a sei mesi dalla data di granulazione.
Il granulato rispetta le caratteristiche tecnico strutturali previste per gli aggregati da riciclo per diverse applicazioni negli allegati C1, C2, C3, C4, C5 alla Circolare Ministeriale n. 5205 del 15/07/2005 "Indicazioni per l'operatività nel settore edile, stradale e ambientale, ai sensi del decreto ministeriale 8 maggio 2003, n. 203", il D.P.R. 21/04/1993, n.246 e il Decreto Ministeriale 9 marzo 1988 n.126 e ss.mm.
Inoltre, per accertare le caratteristiche di fissaggio della matrice inquinante sul granulato, sono stati eseguiti i medesimi test di prova effettuati alla fine della fase di maturazione e post trattamento:

- Indice di appiattimento (frazione > 4 mm) secondo UNI EN 933/3
- Indice di forma (frazione > 4 mm) secondo UNI EN 933/4
- Resistenza alla frammentazione (Los Angeles) secondo UNI EN 1097-6:2002

- Resistenza all'abrasione (Micro-Deval) secondo UNI EN 1097-6:2002
- Contenuto di solfati solubili in acido secondo UNI EN 1744-1:1999
- Contenuto di cloruri solubili in acqua secondo UNI EN 1744-1:1999
- Determinazione dell'influenza di un estratto di aggregato sul tempo di inizio presa del cemento secondo UNI EN 1744-6:2007
- Distribuzione granulometrica e modulo di finezza secondo UNI EN 933-1:1999
- Indice di appiattimento secondo UNI EN 933-3:2004
- Equivalente in sabbia secondo UNI EN 933-8:2000
- Indice di forma secondo UNI EN 933-4:2002
- Dimensione massima Dmax secondo UNI EN 933-1:1999

3. Risultati ottenuti

Nel **secondo periodo** è stato realizzato il dimostratore in ambito geotecnico basato su un sistema di filtrazione configurato con l'impiego di n°4 cisterne da 1000 litri per contenimento di acqua contaminata e acqua filtrata, n 6 fusti in PE da 60 litri collegati in serie per contenimento del mix granulato filtrante, legante idraulico alternativo e terreno, un sistema di pompe e raccorderia idraulica atto a garantire il flusso di acqua in ingresso e in uscita. (foto 1)

Foto 1- sistema di prova filtrazione per acque contaminate

Nel secondo periodo sono stati eseguite valutazioni relative alla stabilizzazione dei terreni mediante l'impiego di aggregati destinati al trattamento acque contaminate. Lo scopo riguarda la valutazione delle prestazioni meccaniche ed adsorbenti nell'impiego combinato di leganti idraulici alternativi e aggregati porosi destinati al trattamento acque.

L'efficacia della soluzione studiata ha dimostrato la possibilità di realizzare, con un singolo intervento di bonifica, l'inertizzazione dei terreni contaminati, la realizzazione di un filtro per il trattamento di acque contaminate, nonché il consolidamento dei terreni tratti con la bonifica.

L'efficacia adsorbente della soluzione sviluppata è dimostrata dai risultati dei test condotti dal CIRCE.

I vantaggi della stabilizzazione dei suoli con aggregati porosi e leganti idraulici alternativi ottenuti con la soluzione sviluppata si possono riassumere in:

- miglioramento delle proprietà geotecniche: l'aggiunta di leganti idraulici ad un aggregato poroso consente di migliorare significativamente le caratteristiche meccaniche del suolo, come la resistenza, la portanza e la stabilità; questo è particolarmente importante per terreni a grana fine che presentano scarse proprietà meccaniche.

- riduzione dei cedimenti: la stabilizzazione di un suolo ne aumenta la resistenza e riduce la sua deformabilità, limitando i cedimenti nel tempo.

- miglioramento del comportamento idrologico: la presenza di un aggregato poroso all'interno della matrice stabilizzata contribuisce a migliorare il drenaggio e la permeabilità del suolo; questo è fondamentale per evitare ristagni idrici e favorire l'infiltrazione dell'acqua.

- immobilizzazione degli inquinanti: i processi di stabilizzazione/solidificazione (S/S) consentono di immobilizzare chimicamente e/o isolare fisicamente gli inquinanti presenti nel suolo; questo avviene attraverso meccanismi di precipitazione, adsorbimento, complessazione e incapsulamento fisico.

- riutilizzo del materiale stabilizzato: il materiale trattato con questa tecnologia può essere riutilizzato in diversi ambiti applicativi, come il riempimento di vuoti di coltivazione mineraria (mine backfill), la realizzazione di rilevati stradali e ferroviari, dune, colline artificiali, riempimenti, ritombamenti e sistemazioni ambientali

- rapidità ed economicità: la stabilizzazione di massa rappresenta un metodo di intervento rapido ed economico, soprattutto quando si interviene su grandi volumi di terreno direttamente in sito.

- flessibilità di applicazione: questa tecnologia può essere applicata sia in situ che ex situ; esistono diverse tecniche di miscelazione del terreno con i leganti, a seconda delle esigenze specifiche del progetto.

Le prestazioni della tecnologia di stabilizzazione dei suoli dipendono da diversi fattori, tra cui:

- caratteristiche dell'aggregato poroso: le caratteristiche dell'aggregato, come la porosità, la granulometria e la composizione chimica, influenzano le prestazioni finali del suolo stabilizzato.

- tipologia di legante idraulico: la scelta del legante dipende dalle caratteristiche del suolo da trattare e dagli obiettivi da raggiungere.

- dosaggio del legante: la quantità di legante utilizzata influenza la resistenza meccanica, la permeabilità e la durabilità del suolo stabilizzato.

- modalità di miscelazione: la miscelazione del terreno con i leganti può avvenire a secco o a umido, in sito o ex situ, con diverse attrezzature; la scelta della tecnica di miscelazione dipende dalle caratteristiche del terreno, dai volumi da trattare e dalle tempistiche del progetto.

OPIGEO avrà la possibilità di industrializzare i risultati ottenuti con il presente progetto, proponendo sul mercato una tecnologia di legante idraulico alternativo adsorbente in grado di migliorare la stabilizzazione meccanica dei terreni.

Sarà affidato ad un fornitore esterno di servizi conto terzi, il compito di macinare e miscelare i diversi ingredienti previsti nella formulazione del legante idraulico alternativo adsorbente, nonché di gestire il confezionamento del materiale pronto alla vendita e lo stoccaggio delle materie prime necessarie da distinta base.

OPIGEO proporrà sul mercato il materiale, supportato da un servizio tecnico di alto livello, necessario per ottimizzare, sui singoli casi specifici, la formulazione del legante e le sue procedure di utilizzo.

In conclusione, i risultati scientifici di maggior rilievo sono riconducibili allo studio condotto da CIRCE, riportato nell'articolo allegato "Stabilization of lead contaminated soil with traditional and alternative binders".
Questo l'articolo descrive i risultati sperimentali di un caso reale di terreno contaminato da Pb trattato con il sistema di solidificazione/stabilizzazione ad alte prestazioni con l'obiettivo di determinare i meccanismi che controllano l'immobilizzazione dei metalli pesanti.
Il processo indagato è un trattamento S/S recentemente progettato specificatamente per la produzione di materiale granulare, che ha lo scopo di facilitare il riutilizzo del terreno trattato come materiale di riempimento o per altri scopi non strutturali.
Sono stati utilizzati tre leganti: un OPC, un cemento all'alluminato di calcio (CAC) e un legante geopolimerico costituito da cemento attivato con NaOH-metacaolino (MK). CAC e MK sono stati studiati come possibili alternative all'OPC, poiché rappresentano un'opzione da utilizzare quando sono coinvolti requisiti di riparazione speciali (nel caso di CAC – per il rapido sviluppo della resistenza) e un modo per ridurre l'impatto ambientale del processo S/S (nel caso di leganti geopolimerici – perché la calcinazione del caolino ha un'impronta di CO2 inferiore rispetto alla produzione di OPC).
Nell'articolo si trova la descrizione dei seguenti argomenti:

- *Campionamento del suolo contaminato*
- *Caratterizzazione del suolo*
- *Ricostruzione dello scenario di contaminazione*
- *Pellettizzazione con OPC*
- *Pellettizzazione con CAC*
- *Pellettizzazione con metacaolino*
- *Risultati sperimentali dell'analisi NMR*
- *Risultati dell'analisi GC-MS*

I risultati complessivi hanno dimostrato che nella ritenzione del Pb sono coinvolti molteplici meccanismi e che i parametri chiave che regolano le prestazioni della stabilizzazione dipendono fortemente dal tipo di sistema legante applicato. Il Pb è risultato associato al C-S-H nel caso dell'OPC, mentre l'ettringite ha svolto un ruolo chiave nella ritenzione di questo contaminante utilizzando il legante CAC. L'uso di un metakaolino attivato con NaOH ha portato a una ritenzione quasi totale del Pb, nonostante la mancanza di solidificazione, evidenziando l'importanza del pH nella regolazione del comportamento di lisciviazione.
Questo studio rappresenta una base conoscitiva importante per sperimentare soluzioni innovative.

4. Ruoli e attività svolta dai partner

L'attività è stata condotta principalmente Opigeo, che ha condiviso e indirizzato la sperimentazione anche su indicazioni e contributi informativi offerti da Chimicambiente ed Elite Ambiente. Il persole delle imprese coinvolto ha potuto condividere la metodologia e i risultati raggiunti.

5. Ruoli e attività svolta dai consulenti

Il consulente **Università di Padova - Circe**, ha condotto lo studio inerente all'uso di tre diversi leganti (OPC, CAC, MK). La Relazione tecnica è stata allegata alla Relazione Intermedia. Nel secondo periodo l'attività di CIRCE non è stata necessaria in quanto nel primo periodo aveva già ottenuto i risultati richiesti.

Documentazione fotografica, schemi

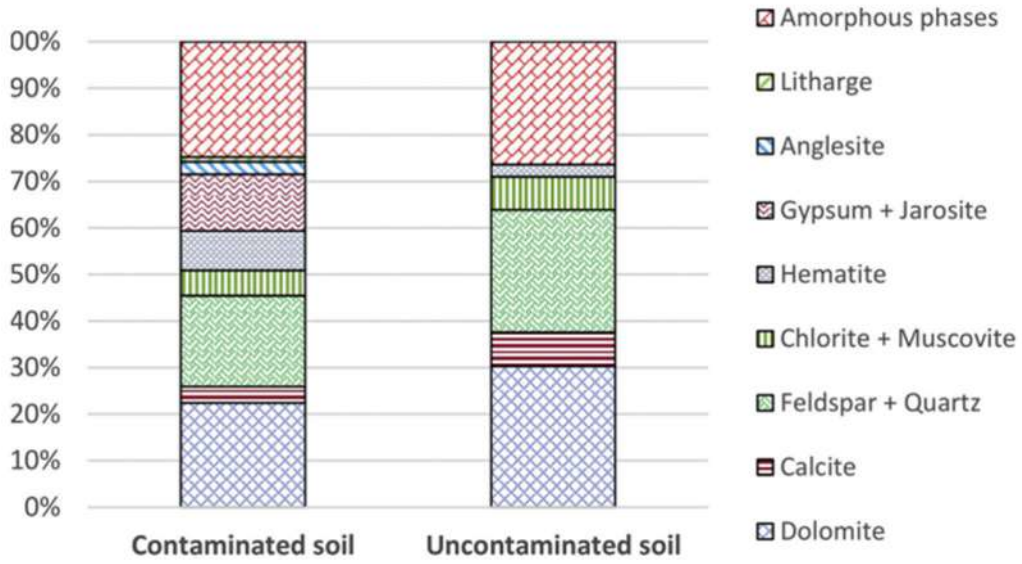

Fig. 1. Mineralogical composition of contaminated and uncontaminated soil obtained by XRD quantitative analysis.

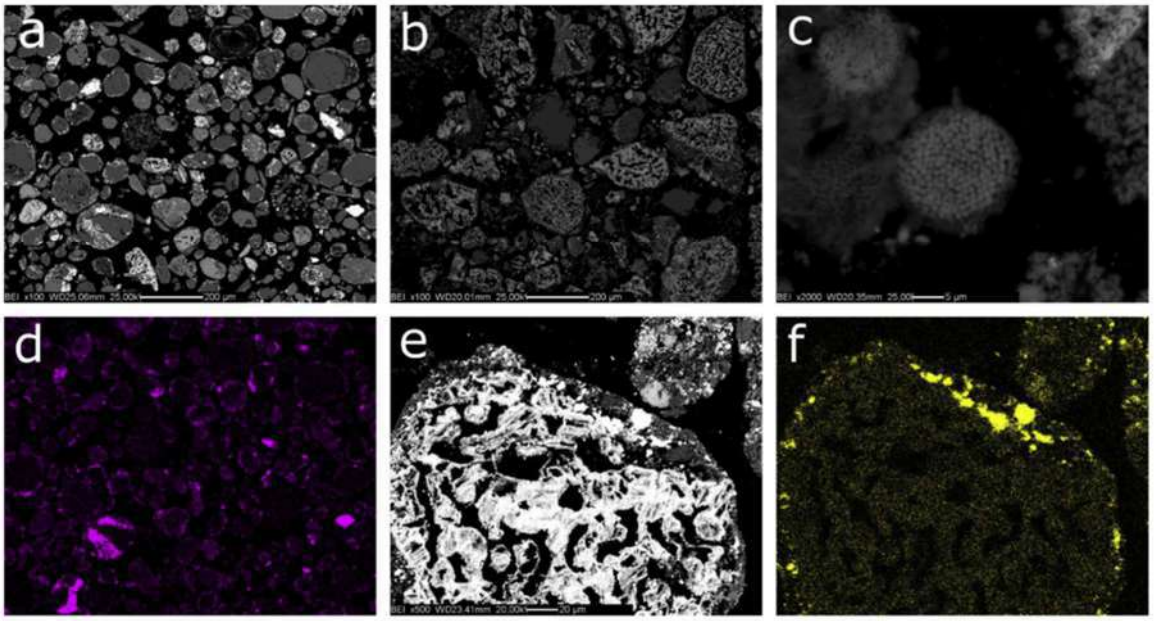

Fig. 2. SEM micrographs of the contaminated soil. (a) Back-scattered electron image of the bulk soil; (b) back-scattered electron image of the material sampled from the purple layer, showing a large amount of iron oxides; (c) back-scattered electron image of framboidal pyrite found in the light yellow layer; (d) map of the Pb distribution relative to image (a); (e) iron oxide particle; and (f) Pb mapping showing the metal adsorption on the particle in image (e). (For interpretation of the references to colour in this figure legend, the reader is referred to the web version of this article).

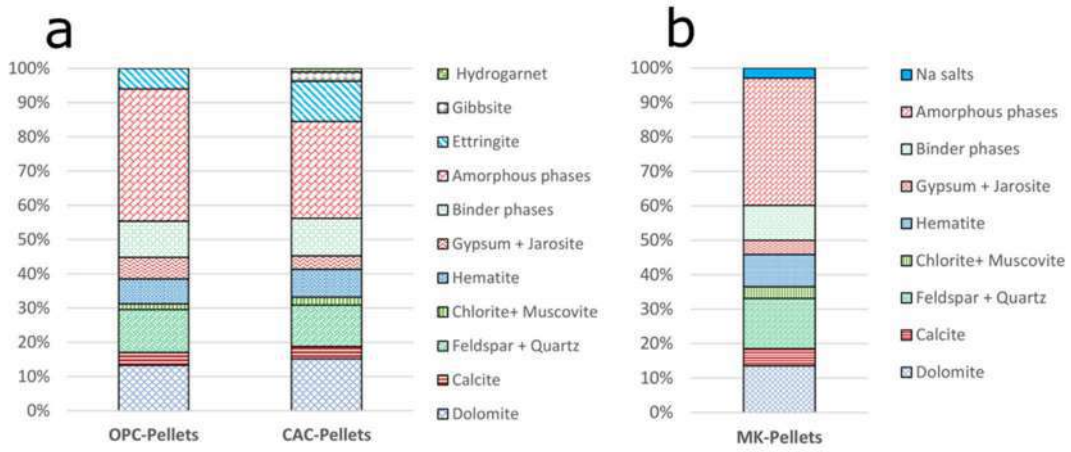

Fig. 3. Mineralogical compositions of OPC-pellets (a), CAC-pellets (a) and MK-pellets (b) expressed as weight percent (w.t.%) for every phase. Binder phases encompass unreacted clinker phases. Amorphous phases in OPC and CAC-pellets are constituted both by the amorphous fraction of soil and the newly formed amorphous hydration products. Amorphous phases in MK-pellets are the sum of the amorphous fraction of soil, the amorphous metakaolin and the newly formed geopolymeric products.

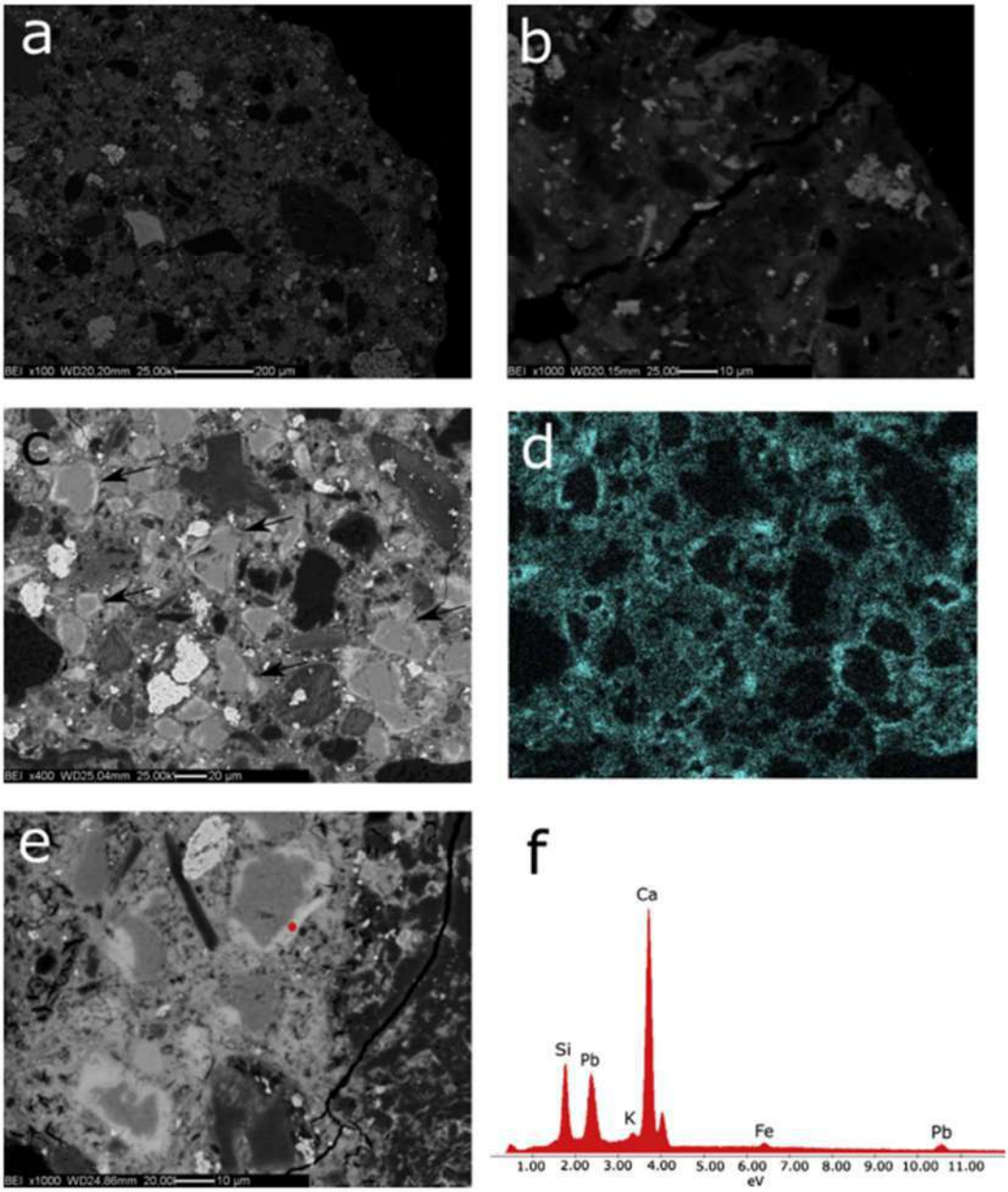

Fig. 4. SEM micrographs of polished sections of OPC-pellets. (a) Internal microstructure with soil particles embedded within the amorphous matrix given by cement; (b) soil particles dissolving in the alkaline medium; (c) internal microstructure showing unhydrated clinker particles (arrows); (d) map of Pb relative to image c obtained by choosing only the Pb signal at 10.5 eV to exclude S interferences; (e) high magnification image showing cement particles surrounded by a Pb-rich white halo; and (f) EDX spectrum correspondent to the red point in image (e). (For interpretation of the references to colour in this figure legend, the reader is referred to the web version of this article).

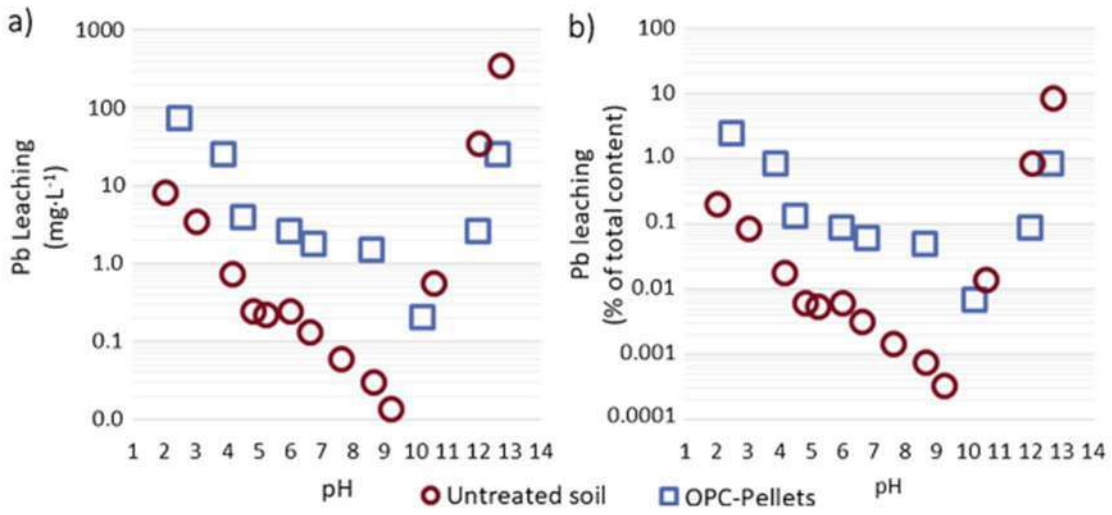

Fig. 5. Pb leaching as a function of pH – comparison of untreated soil and OPC-pellets. The release is expressed as mg·L^{-1} of Pb in the eluate (a) and as percentage of leached Pb with respect to total amount in the starting material (b).

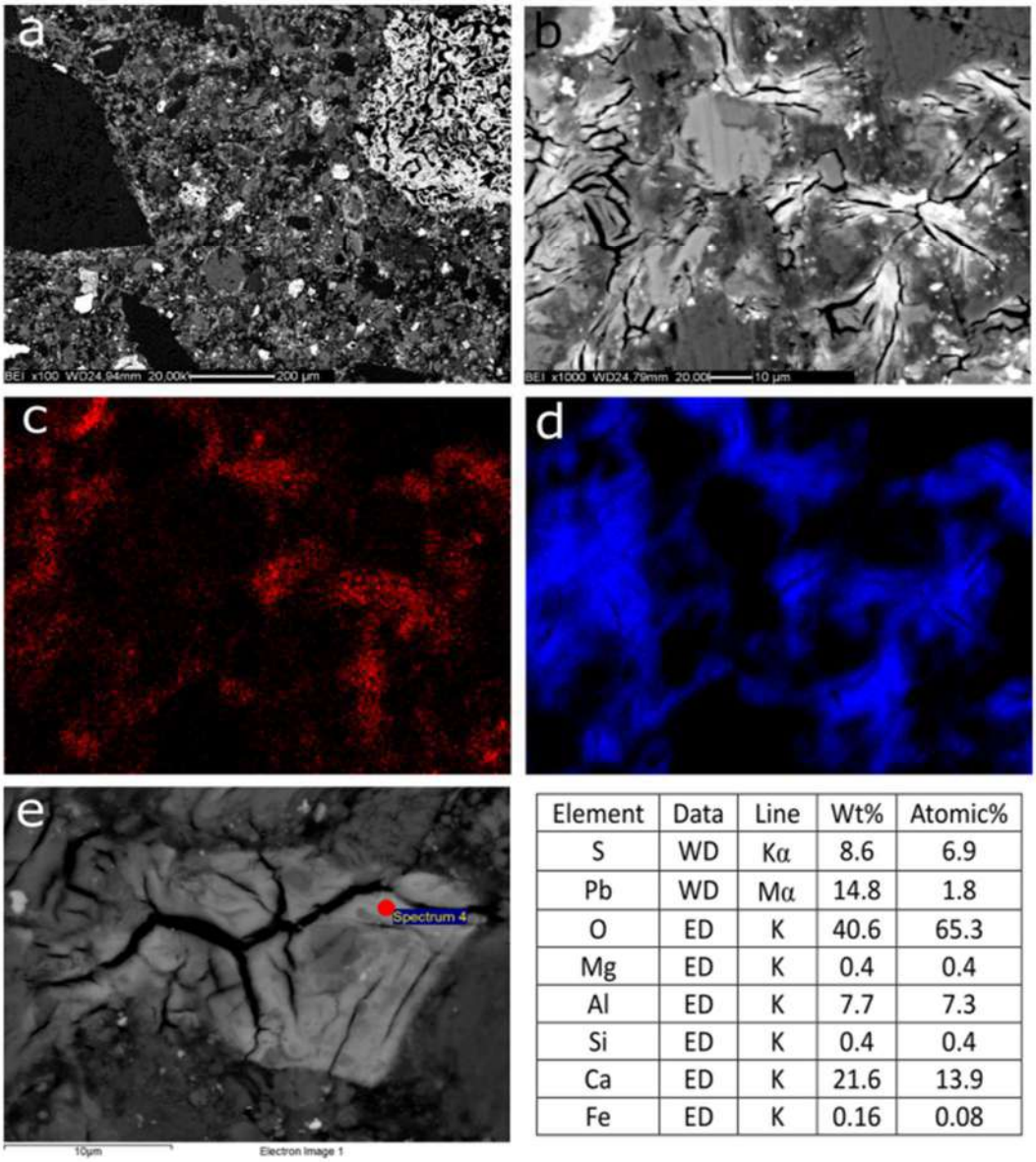

Element	Data	Line	Wt%	Atomic%
S	WD	Kα	8.6	6.9
Pb	WD	Mα	14.8	1.8
O	ED	K	40.6	65.3
Mg	ED	K	0.4	0.4
Al	ED	K	7.7	7.3
Si	ED	K	0.4	0.4
Ca	ED	K	21.6	13.9
Fe	ED	K	0.16	0.08

Fig. 6. SEM micrographs of polished sections of CAC-pellets. (a) Internal microstructure; (b) Internal microstructure at higher magnification showing the cracks for the dehydration of ettringite in the high vacuum conditions; (c) map of Pb relative to image (b); (d) map of S relative to image (b); (e) FESEM image of ettringite with the chemical composition of the red point reported (WD = wavelength dispersive, ED = energy dispersive). (For interpretation of the references to colour in this figure legend, the reader is referred to the web version of this article).

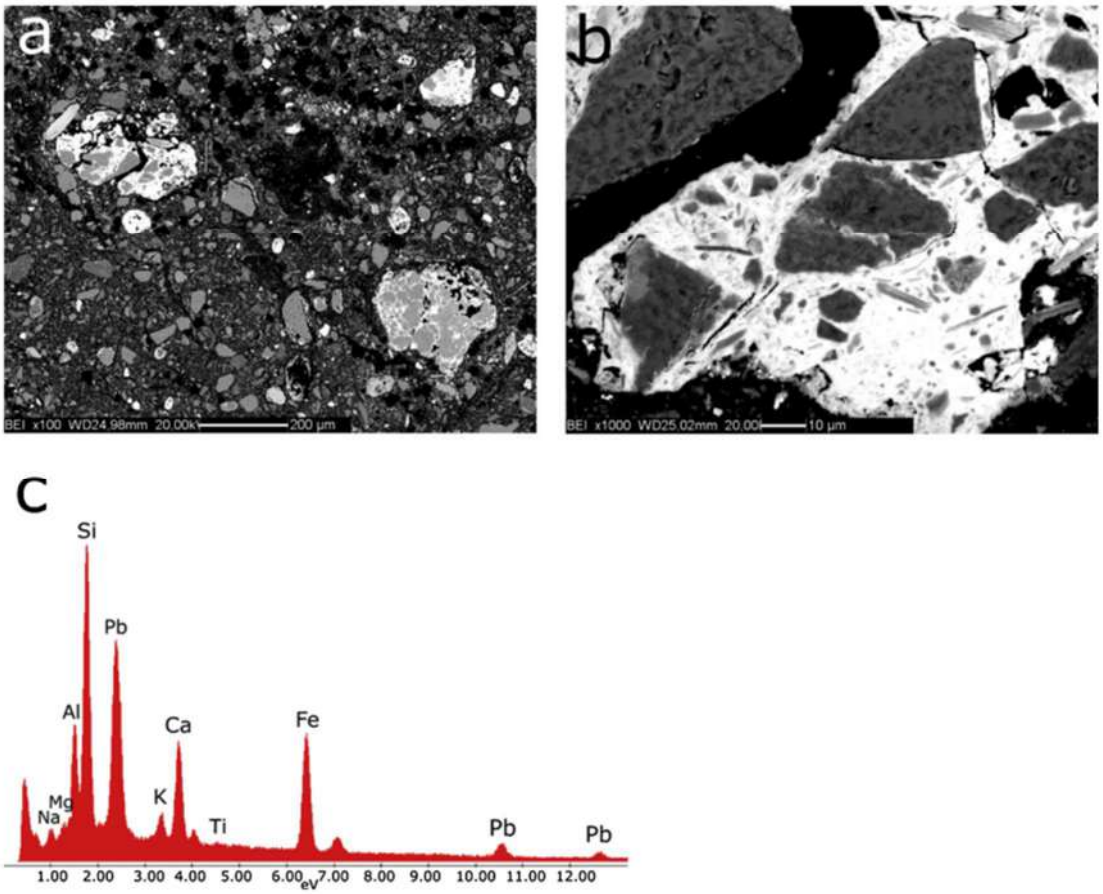

Fig. 7. SEM micrographs of the polished sections of MK-pellets. (a) Internal microstructure showing high porosity and light gray/white aggregates; (b) aggregate composed of soil phases (gray) embedded in a matrix (white); and (c) elemental composition of the white-colored phase in image (b).

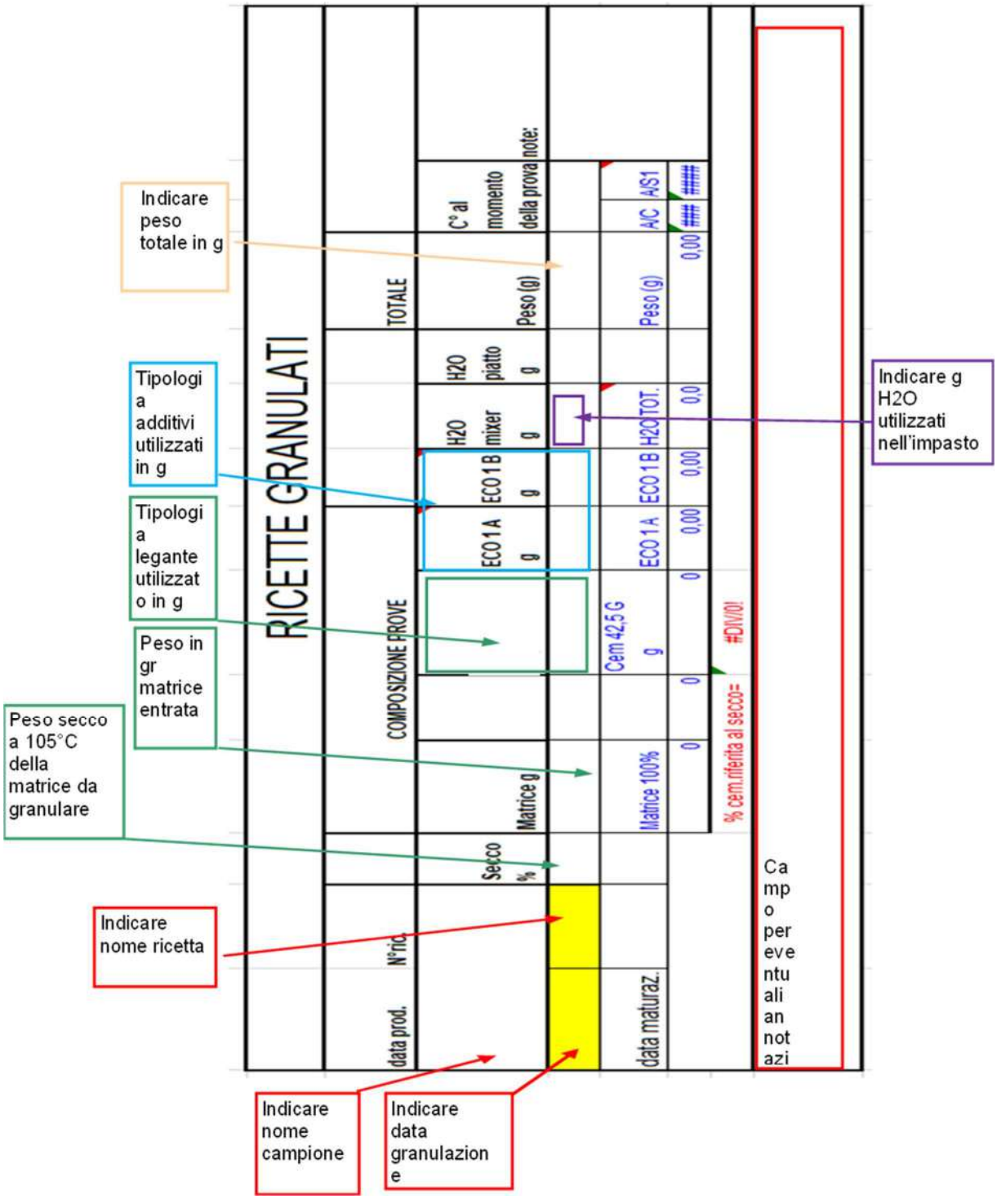
RICETTE GRANULATI
TOTALE
COMPOSIZIONE PROVE
Secco %
Matrice g
ECO1A g
ECO1B g
H2O mixer g
H2O piatto g
Peso (g)
C° al momento della prova
note:
N°ric.
data prod.
Matrice 100%
Cem 42,5 G g
ECO 1.A
ECO 1.B
H2OTOT.
Peso (g)
A/C
A/S1
% cem.riferita al secco=
#DIV/0!
data maturaz.
Campo per eventuali annotazi
Indicare peso totale in g
Tipologia additivi utilizzati in g
Tipologia legante utilizzato in g
Peso in gr matrice entrata
Peso secco a 105°C della matrice da granulare
Indicare nome ricetta
Indicare nome campione
Indicare data granulazione
Indicare g H2O utilizzati nell'impasto

Tabella 1. Set analitico per le analisi sul tal quale

PARAMETRI FISICI	SOSTANZE ORGANICHE
Rame (Cu)	
Mercurio (Hg)	
Nichel (Ni)	
Piombo (Pb)	
Selenio (Se)	
Zinco (Zn)	
Cromo esavalente (Cr VI)	
Tellurio (Te)	
Tallio (Tl)	
Stagno (Sn)	
Berillio (Be)	
Cobalto (Co)	
Vanadio (V)	

Tabella 2. Set analitico per le analisi mediante test di cessione

Nitrati (ione nitrato)
Fluoruri (ione fluoruro)
Solfati (ione solfato)
Cloruri (ione cloruro)
Cianuri totali (ione cianuro)
Bario
Rame
Zinco
Berillio
Cobalto
Nichel
Vanadio
Arsenico
Cadmio
Cromo totale
Piombo
Selenio
Mercurio
Amianto
COD
pH

Tabella 3. Set analitico per le analisi sul tal quale

PARAMETRI FISICI	SOSTANZE ORGANICHE
Aspetto fisico	Carbonio organico totale (TOC)
Residuo a 105 °C	Solventi organici aromatici
Residuo a 600 °C	Solventi organici clorurati
pH	Solventi organici volatili
METALLI PESANTI	Policlorobifenili totali (PCB)
Arsenico (As)	Speciazione classi idrocarburiche
Antimonio (Sb)	Idrocarburi leggeri (C<12)
Cadmio (Cd)	Idrocarburi pesanti (C>12)
Cromo (Cr)	Idrocarburi Policiclici Aromatici (IPA)
Rame (Cu)	
Mercurio (Hg)	
Nichel (Ni)	
Piombo (Pb)	
Selenio (Se)	
Zinco (Zn)	
Cromo esavalente (Cr VI)	
Tellurio (Te)	
Tallio (TI)	
Stagno (Sn)	
Berillio (Be)	
Cobalto (Co)	
Vanadio (V)	

Tabella 4. Set analitico per le analisi mediante test di cessione

Nitrati (ione nitrato)
Fluoruri (ione fluoruro)
Solfati (ione solfato)
Cloruri (ione cloruro)
Cianuri totali (ione cianuro)
Bario
Rame
Zinco
Berillio
Cobalto
Nichel
Vanadio
Arsenico
Cadmio
Cromo totale
Piombo
Selenio
Mercurio
Amianto
COD
pH

CIRCe

CENTRO INTERDIPARTIMENTALE DI RICERCA PER LO STUDIO DEI MATERIALI CEMENTIZI E DEI LEGANTI IDRAULICI - CIRCe

UNIVERSITÀ DEGLI STUDI DI PADOVA

Progetto INERTEX

FONDI FSC 2014-2020_Bando Aggregazioni DGR 1800 del 15/12/2021, n°10439274, CUP:B69J22002990009

PSC FSC 2014 2020 SEZIONE SPECIALE
PIANO SVILUPPO E COESIONE - VENETO

COMMITTENTE	Opigeo srl
DOCUMENTO	Rapporto Tecnico/Relazione intermedia
DATA	16/10/2023
TITOLO	**Stabilization of lead contaminated soil with traditional and alternative binders**
ABSTRACT IT	L'applicazione di un innovativo processo di solidificazione/stabilizzazione (S/S) è stata studiata per la bonifica di terreni contaminati da Pb. Le prestazioni della stabilizzazione del Pb sono state valutate confrontando l'uso di cemento alluminato di calcio (CAC) e di un legante metakaolino attivato con alcali rispetto al cemento Portland ordinario (OPC). La composizione di fase dei prodotti stabilizzati è stata analizzata mediante XRD e correlata alla microstruttura interna ottenuta mediante immagini SEM-EDX. Sono stati eseguiti test di lisciviazione per accertare l'effcacia dei leganti proposti nella S/S del terreno contaminato e il rilascio di Pb è stato valutato per ciascun sistema legante. I risultati complessivi hanno dimostrato che nella ritenzione del Pb sono coinvolti molteplici meccanismi e che i parametri chiave che regolano le prestazioni della stabilizzazione dipendono fortemente dal tipo di sistema legante applicato. Il Pb è risultato associato al C-S-H nel caso dell'OPC, mentre l'ettringite ha svolto un ruolo chiave nella ritenzione di questo contaminante utilizzando il legante CAC. L'uso di un metakaolino attivato con NaOH ha portato a una ritenzione quasi totale del Pb, nonostante la mancanza di solidificazione, evidenziando l'importanza del pH nella regolazione del comportamento di lisciviazione.
Firma del responsabile	Per il Centro CIRCe La Direttrice Prof.ssa Maria Chiara Dalconi

1. Introduction

Soil contamination due to the presence of heavy metals is efficiently treated with immobilization-based technologies such as solidification/stabilization (S/S) (Mulligan et al., 2001). Solidification/stabilization process encompasses both chemical immobilization of the contaminants and physical stabilization of the soil by reacting the contaminated matrix with a hydraulic binder (typically Ordinary Portland Cement, OPC) (Batchelor, 2006). However, despite the well-understood chemistry of OPC as a building material, the mechanisms that control the immobilization of heavy metals in cement-soil systems are not well established. According to theory, S/S with cement results in the precipitation or coprecipitation of metal ions as hydroxides or in their uptake by cement hydration products, e.g., in calcium silicate hydrate, or ettringite and/or monosulfate-type phases (Gougar et al., 1996; He and Suito, 2008; Li et al., 2019). However, experimental attempts to prove this theory do not provide comprehensive ex-post direct evidence of such immobilization mechanisms but, in most cases, refer to ex-ante synthesis and characterization of prepared materials (Li et al., 2019; Wang et al., 2018a; Wang et al., 2019; Chen et al., 2009; Bakhshi et al., 2019; Su et al., 2016; Li et al., 2014). The occasional formation of new mineralogical phases containing toxic metallic cations or oxyanions has been reported (Wang et al., 2018a; Wang et al., 2018b; Guo et al., 2017a; Lv et al., 2016; Zhang et al., 2018), but the role of these phases in the retention of toxic elements is not always evident and clear. Many studies have been published regarding the hydration of metal-doped OPC or single cement phases (Zhang et al., 2018; Niu et al., 2018; Vollpracht and Brameshuber, 2016; Lu et al., 2019; Ahn et al., 2014), but although highly informative in assessing the effect of different hazardous elements on hydration reactions and leaching properties, these studies are hardly representative of real contamination conditions. This paper reports experimental results of a real case of Pb-contaminated soil treated with the High Performance Solidification/Stabilization (HPSS®) process (Scanferla et al., 2009) with the aim to determine the mechanisms that control the immobilization of heavy metals. The HPSS® process is a recently engineered *ex situ* S/S treatment specifically addressed to granular material production, which is intended to facilitate the reuse of treated soil as filling material or for other nonstructural purposes. Three binders were employed: one OPC, one calcium aluminate cement (CAC) and a geopolymeric binder made of NaOH-activated metakaolin (MK). CAC and MK were investigated as possible alternatives to OPC, since they are an option for use when special remediation requirements are involved (in the case of CAC – for its fast strength development) and a way for lowering the environmental impact of the S/S process (in the case of geopolymeric binders – because kaolin calcination has a lower CO_2 footprint than OPC production). Few studies have evaluated the application of CAC for stabilizing heavy metals (Bougharraf et al., 2018; Voglar and Leštan, 2013; Ivanov et al., 2016; Falzone et al., 2015), while the theoretical feasibility of applying geopolymers as binding agents for toxic metals has long been a topic of study (van Jaarsveld et al., 1997; Shi and Fernández-Jiménez, 2006) with most recent publications dealing with slag or fly ash-based geopolymers (Mao et al., 2019; Zhang et al., 2017a; Arnold et al., 2017; Guo et al., 2017b; Fansuri et al., 2019; Daniil et al., 2018; Koplík et al., 2018; Fernández-Pereira et al., 2018; Zhang et al., 2019) and more limited examples of applications of calcined clays (Joussein et al., 2019; Łach et al., 2018). In this work, the effects of different binders on S/S performance are presented and discussed.

2. Experimental

2.1. Contaminated site and soil sampling

One cubic meter of soil was excavated from a brownfield located in an abandoned production and storage site located in Bagnolo Mella (BS, Italy). This industrial site devoted to fertilizer production, operational between 1898 and 1985, included a sulfuric acid production plant by means of pyrite (FeS_2) roasting process. The contaminated soil sample was collected from the surface to 1.5 m depth, air-dried up to 10% weight/weight (w/w) moisture content and sieved at 2 mm prior to homogenization, as in the already established HPSS® industrial procedure (Scanferla et al., 2009). The sampled soil was an unsaturated soil mainly composed of sandy-gravelly material, as determined by the geological survey prior to the reclamation activities. At the same time, subsamples of different layers of the subsoil were collected with the sampling criterion being variation in color. This allowed us to distinguish an upper layer with bricks and other debris (layer a), an underlying zone composed of a purple layer (layer b), a light-yellow layer with pale brown intercalations (layer c), and a brown-colored layer (layer d) (Figure S1). A sample of soil was collected in an area that was found not contaminated according to the regulatory limits imposed by the Italian regulation for the use of soil and sediments for industrial purposes (Enviromental Ministry Decree EMD, 2006). This sample was used to represent the mineralogical composition of the soil prior to contamination, and it was collected at a depth between 15 and 35 cm, air-dried, sieved at 2 mm and characterized.

2.2. Binders

Three binding systems were tested for the solidification/stabilization of the contaminated soil: an Ordinary Portland Cement (OPC) (CEM I 52.5 R, from Barbetti S.p.A., Gubbio, Italy), a calcium aluminate cement (CAC)(Gorkal 70, from Mapei S.p.A., Milano, Italy) and a metakaolin (MK)(Argical 1000, from Bal-Co, Sassuolo, Italy) activated by a 4 M NaOH solution, which was obtained by dissolving pellets of NaOH (ACS Reagent, Merck KGaA, Darmstadt, Germany) in ultrapure water. The mineralogical compositions of the binders are reported in Table S1. Two water-reducing additives (Mapeplast ECO 1-A and Mapeplast ECO-1B) were purchased from Mapei S.p.A., (Milan, Italy). Ultrapure water with a resistivity of 18.2 MWcm was obtained with MilliQ system from Merck KGaA (Darmstadt, Germany).

2.3. Pelletization

The HPSS® technology was applied to the contaminated soil after air-drying and sieving by adapting at lab-scale the procedure developed by Bonomo and co-workers (Bonomo et al., 2009). The soil and binders were blended for 5 min in a mechanical mixer with the proper amount of tap water or NaOH solution to prevent the formation of dust aerosols, depending on whether the binder was cement or metakaolin, respectively. Two water-reducing additives (Mapeplast ECO 1-A and Mapeplast ECO-1B) were added, each as 2% of cement dry weight. Mapeplast ECO 1-A is a hydrophobic additive that is used to decrease concrete water adsorption, whereas Mapeplast ECO 1-B is an acrylic-based superplasticizer that is used to better disperse cement particles. Since such additives are designed for use in traditional cement/concrete (Ferrari et al., 2010) and are known to degrade rapidly in the alkaline solution of geopolymers (Nematollahi and Sanjayan, 2014), they were included exclusively in the OPC and CAC formulations. Then, the mixture was poured into a laboratory granulator plate, where additional water or NaOH solution was added to promote the granulation process until the development of millimeter-sized pellets. The water-to-cement ratio was in the range of 0.5 – 0.6, whereas the NaOH solution-to-MK ratio was 0.9 because of the higher water demand of MK. About 5% of each solution (i.e. water and NaOH solution) was added during mixing to prevent the formation of dust aerosol, while the remaining was added during the pelletization stage. The S/S recipe was fixed, including 73% dry weight/dry weight (d.w./d.w.) of soil (having 10% humidity content) and 27% (d.w./d.w.) of dry binder. The pellets were cured in sealed plastic bags at ambient temperature for 28 days, then sieved following the UNI EN 933-1 standard (British Standards Institution, 2005). The fraction of pellets with diameters between 2 and 10 mm was

considered for this study. This range of particle sizes is normally produced during industrial scale applications of the HPSS® process, while pellets outside this range are reprocessed after milling.

2.4. X-ray diffraction (XRD), X-ray fluorescence (XRF) and scanning electron microscopy equipped with energy-dispersive X-ray spectrometry (SEM/EDX)

The mineralogical composition of powdered samples was determined quantitatively by Rietveld analysis of XRD data. Known amounts of ZnO internal standard (ACS Reagent, Thermo Fisher Scientific Inc., Waltham, MA, USA) were mixed to the samples to quantify the amorphous fractions. Diffraction data were acquired with a X'Pert Pro diffractometer (Malvern Panalytical, Malvern, UK) according to the measurement details reported in Table S2. The elemental composition of the contaminated soil was determined with XRF spectrometry using a Wavelength Dispersive Sequential (WDS) Philips PW2400 spectrometer (Spectris, Egham, UK). Instrumental precision and detection limits are reported in Table S3. Internal microstructure investigations on polished and carbon-coated sections of pellets were performed using a CamScan MX3000 SEM (Applied Beams, Beaverton, OR, USA) equipped with an EDX spectrometer. Samples were dry-polished to avoid further hydration of cement phases and dissolution of the most soluble species. Care was taken in the polishing process by continuously removing the residues on the abrasive papers, to avoid the formation of scratches on the samples surface. Standard-less elemental mapping and point analyses were performed, and the images were processed with ImageJ software (U.S. National Institutes of Health – NIH). An additional detailed investigation on CAC-pellets microstructure was performed using a Merlin™ Field Emission Scanning Electron Microscope (FESEM) (Carl Zeiss, Oberkochen, Germany), equipped with a wavelength dispersive spectrometer (WDS) for elemental analysis. For the quantitative analysis of Ca, Al, S, O, Pb, Mg, Fe, C and Si the following standards were used: FeS_2, $PbMoO_4$, $CaCO_3$, $CaMgSi_2O_6$ and $KAlSi_3O_8$.

2.5. Inductively coupled plasma mass spectrometry (ICP-MS)

ICP-MS analysis was conducted to determine heavy metal concentrations in eluates from leaching tests and on solid samples using a NexION 350D spectrometer (Perkin Elmer, Waltham, MA, USA), which was operated in standard mode, collision mode (Kinetic Energy Discrimination, KED) and reaction mode (Dynamic Reaction Cell, DRC) (Table S4). The choice of the optimal acquisition mode was dictated by the severity of the polyatomic interferences for each analyte to reach the lowest detection limit for each element. Solid samples were digested in accordance to the procedure reported by Bettiol and coworkers (Bettiol et al., 2008). HNO_3, HF, HCl and H_3BO_3 (AppliChem GmbH, Darmstadt, Germany) were used at high purity level for trace metal analyses. NIST-SRM 2711a (Montana II Soil) from NIST (National Institute of Standards and Technology, Gaithersburg, MD, USA) was used as a certified standard to validate the analytical methodology. All instrumental settings are reported in Table S5. All analyses were performed in triplicate.

2.6. Leaching tests

Leaching tests were performed on treated and untreated soil following the UNI 12457-4:2004 (British Standards Institution, 2004) and the UNI 14429:2015 (British Standards Institution, 2015) standards. The first one is a batch leaching test in ultrapure water, whereas the UNI 14429:2015 consists of a series of parallel batch extractions with an increasingly acid or basic leachant, prepared using nitric acid or sodium hydroxide (semiconductor grade > 99.99%, Merck KGaA, Darmstadt, Germany). This leaching test was used to investigate the release of Pb relative to the pH of the leachant. While the first test was conducted on all materials studied, the second method was applied only on OPC-pellets and untreated soil. Each material was analyzed in triplicate after applying coning and quartering to obtain adequate samples. Eluates were filtered at 0.45 μm and were analyzed for heavy metals by ICP-MS and for pH. The pH values of the eluates obtained from the UNI 12457-4:2004 leaching test were considered as the characteristic pH values of each material because this test was designed to reach equilibrium conditions in a neutral solvent.

3. Results and discussion

After a detailed chemical and mineralogical characterization, the contaminated soil was pelletized with the selected binders (i.e. OPC, CAC and MK) to obtain stabilized granular materials. The mineralogical composition, microstructure and leaching behavior of these products were investigated. Since Pb is the only heavy metal present in the contaminated soil at high enough concentration to be identified by XRD and SEM-EDX mapping, only its leaching was considered in this work. The results are detailed below.

3.1. Soil characterization

The mineralogical composition of the homogenized sample of contaminated soil is reported in Fig. 1 and Table S6, together with the mineralogy of the uncontaminated soil sample collected outside the contaminated area. The results of XRF analysis performed on the contaminated soil are reported in Table S7. The heavy metal content of the polluted soil is presented in Table S8, showing a very high

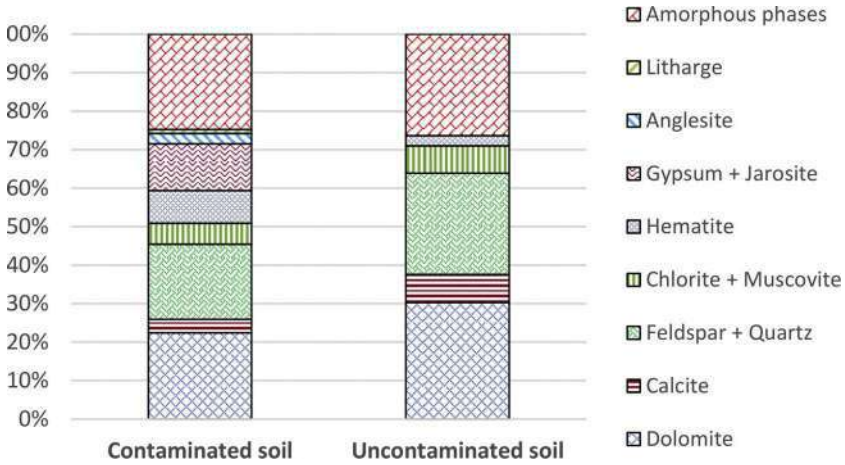

Fig. 1. Mineralogical composition of contaminated and uncontaminated soil obtained by XRD quantitative analysis.

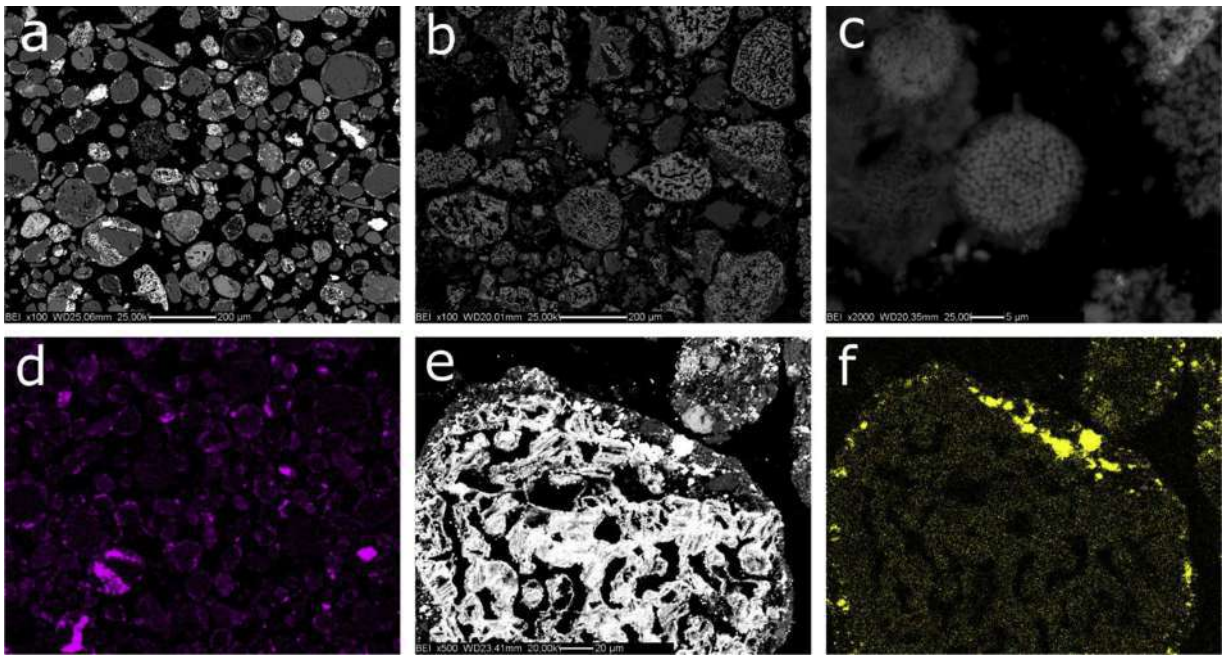

Fig. 2. SEM micrographs of the contaminated soil. (a) Back-scattered electron image of the bulk soil; (b) back-scattered electron image of the material sampled from the purple layer, showing a large amount of iron oxides; (c) back-scattered electron image of framboidal pyrite found in the light yellow layer; (d) map of the Pb distribution relative to image (a); (e) iron oxide particle; and (f) Pb mapping showing the metal adsorption on the particle in image (e). (For interpretation of the references to colour in this figure legend, the reader is referred to the web version of this article).

concentration of Pb (40430 ± 3210 mg·kg^{-1}), together with minor amounts of As (383 ± 24 mg·kg^{-1}) and Se (362 ± 28 mg·kg^{-1}).

Soil mineralogy was a combination of primary components (i.e., the aluminosilicate, silicate and carbonate minerals initially present in the soil) and secondary phases that were produced by the industrial activities and weathering processes in the area, namely hematite (Fe_2O_3), gypsum ($CaSO_4{\cdot}2(H_2O)$), anglesite ($PbSO_4$) and jarosite ($KFe^{3+}_3(SO_4)_2(OH)_6$). Since the amorphous fraction of soil accounted for one fourth of the composition, an attempt to characterize such phase was made. The comparison between the chemical composition of the crystalline fraction of soil calculated by XRD quantitative analysis and the bulk chemical composition of soil obtained with XRF analysis yielded information about the nature of the amorphous fraction of the soil. These results, reported in Table S9, indicated a chemical composition resembling iron oxides and aluminosilicate minerals. SEM/EDX images of the contaminated soil are displayed in Fig. 2.

A detailed analysis of the sample from the purple layer (layer b) revealed a large number of Fe phases, possibly hematite, jarosite and amorphous iron oxides, the latter being residues of the pyrite roasting process (Fig. 2b). Sulfate-containing phases were also detected and were identified as gypsum and natrojarosite ($NaFe^{3+}_3(SO_4)_2(OH)_6$) on the basis of the information derived from XRD data. The underlying light-yellow layer (layer c) was mainly composed of gypsum, jarosite and natrojarosite. In this layer, SEM images showed the presence of some framboidal pyrite particles (Fig. 2c) that have not yet been oxidized. The lower investigated layer (layer d) contained many aluminosilicate minerals as well as carbonates and silicon oxide and seemed to be mostly untouched by contamination. XRD quantitative analyses of layers b, c and d are reported in Table S10.

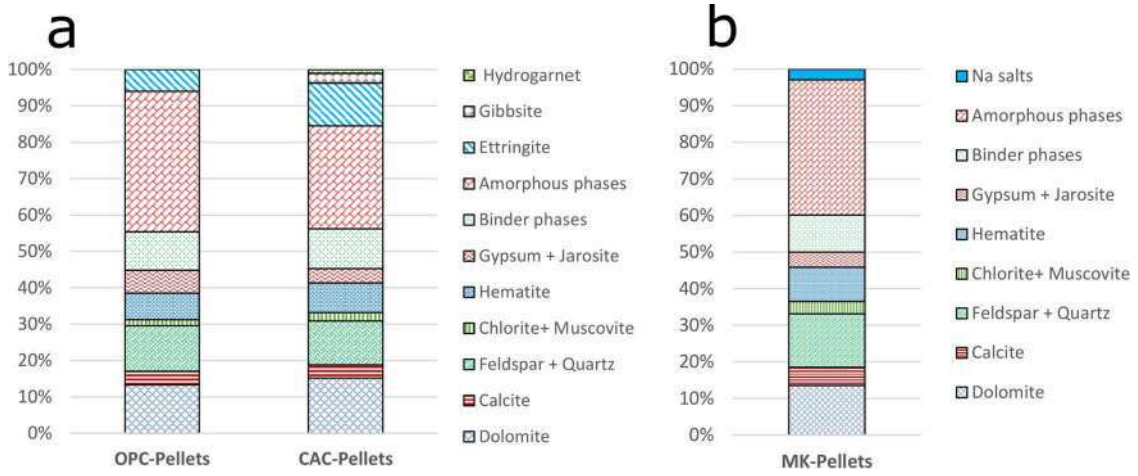

Fig. 3. Mineralogical compositions of OPC-pellets (a), CAC-pellets (a) and MK-pellets (b) expressed as weight percent (w.t.%) for every phase. Binder phases encompass unreacted clinker phases. Amorphous phases in OPC and CAC-pellets are constituted both by the amorphous fraction of soil and the newly formed amorphous hydration products. Amorphous phases in MK-pellets are the sum of the amorphous fraction of soil, the amorphous metakaolin and the newly formed geopolymeric products.

3.2. Reconstruction of the contamination scenario

In the investigated area, pyrite was present as a raw material for sulfuric acid manufacturing. It is well-known that the oxidation of sulfide minerals can lead to acid sulfate water production (Bigham and Nordstrom, 2011). The resulting acidity can be considered the main reason for the mobilization of heavy metals in the studied soil, similarly to what is observed during acid mine drainage (Akcil and Koldas, 2006). These conditions led to the precipitation of minerals in the soil that are typically found in acid sulfate soils, such as sulfates and hydroxysulfates. Jarosite is one of these phases and it was abundant in the light-yellow layer of the contaminated soil. Jarosite forms in a pH range of 1–3 (Stoffregen et al., 2011). Other phases having similar behaviors are gypsum and anglesite, which together accounted for more than 13% of the bulk soil mineralogy. The pH of the contaminated sample (7.5) showed how the high amount of carbonate minerals (26% of soil mineralogy) contributed to neutralization of soil acidity. The remarkable concentration of Pb found in the contaminated soil can be related to the use of lead-lined ovens and Pb-rich raw materials for sulfuric acid manufacturing. Lead is highly enriched in pyrite ores (ranging from 813 to 11377 mg kg^{-1} with an average of 4030 mg kg^{-1}) compared to lead abundance in Earth's crust, that is limited to 10 mg kg^{-1} (Aguilar-Carrillo et al., 2018). Additionally, galena (PbS) has been reported as a Pb host in pyrite ores (Yang et al., 2009). Due to pyrite oxidation, it is likely that the acid Fe^{III}-rich solution promoted the dissolution of galena, as reported in the following reaction:

$$PbS + 2Fe^{3+} + 3SO_4^{2-} + \frac{3}{2}O_2 + H_2O \rightarrow PbSO_4 + 2Fe^{2+} + 2H^+ + 3SO_4^{2-} \quad (1)$$

leading to formation of anglesite, which is very weakly soluble in acidic conditions (Dove and Czank, 1995). In addition to anglesite, Pb was also found adsorbed onto the amorphous iron oxide particles (Fig. 2e, f).

3.3. Pelletization with OPC

XRD analysis of OPC-pellets after 28 days of curing (Fig. 3a and Table S11) showed the presence of soil phases and cement phases, both hydrated and unhydrated. The comparison of XRD patterns of contaminated soil and OPC-pellets (Figure S2) showed that Pb-containing minerals (i.e., anglesite) were completely dissolved by the high pH values reached after mixing with cement. Measure of pH of the eluate at the end of the UNI 12457-4 leaching test indicated a value of 12.3. No newly formed crystalline phases containing Pb were detected by XRD analysis in the OPC-pellets. Also gypsum, initially detected in the soil, was consumed leading to the formation of ettringite ($Ca_6Al_2(SO_4)_3(OH)_{12}{\cdot}26(H_2O)$), one of the first products that forms during cement hydration (Lea, 2004). While ettringite normally forms in purely cementitious systems because of the reaction between calcium aluminates and sulfates in the presence of water, in this hybrid system composed of soil and cement, ettringite may also precipitate from the dissolved sulfate ions derived from the dissolution of gypsum and anglesite, which were present in the contaminated soil. Even if not directly detectable by the presence of diffracted Bragg peaks (because of their amorphous structures), calcium silicate hydrates (C-S-H phase) were present in OPC-pellets based on quantitative analysis with internal standard and quantified as ca. 20% of the bulk pellet. This percentage was calculated by subtracting the amorphous counterpart present in soil from the entire amorphous fraction in the OPC-pellet. The C-S-H phase in OPC is formed by reaction of tricalcium silicates (Ca_3SiO_5, abbreviated C_3S) with water through a dissolution process liberating calcium and silicate ions in solution followed by the precipitation of the C-S-H phase on C_3S surfaces (Taylor, 2003).

Portlandite ($Ca(OH)_2$ or CH according to cement chemistry notation), which normally forms after C_3S hydration, was not detected in the OPC-pellets. It is likely that the pore solution did not reach the level of Ca^{2+} saturation required for CH precipitation as a consequence of pozzolanic reactions between Ca^{2+} and siliceous counterparts derived by the dissolution of amorphous silica, leading to additional C-S-H precipitation. Amorphous silica, which was likely included in the amorphous fraction of soil, is known to increase its dissolution kinetics at a pH above 9 (Krauskopf, 1956). The considerable amount of unhydrated cement (37% of the total added cement) indicates a limited hydration degree of cement paste. Normally after 28 days of curing, the percentage of unhydrated OPC is approximately 5–15% (Chen et al., 2009). Despite this, the amount of C-S-H phase found was relatively high, supporting the hypothesis of pozzolanic reactions producing additional C-S-H. The drastic deceleration of clinker hydration was particularly true for the C_3A and C_2S phases, whose amounts were almost the same as the pre-hydration scenario. While C_2S is known to have slow hydration kinetics, C_3A is rapidly reactive with water (Taylor, 2003). The simultaneous presence of C_3A and ettringite - the latter normally forming upon C_3A dissolution - suggests that other aluminum suppliers were dissolving, yielding aluminate ions for ettringite formation. It is suggested that clay minerals with particle sizes < 0.2 μm were likely included in this amorphous counterpart of soil, and that their dissolution in the alkaline pH induced by cement could have supplied aluminate ions. The internal microstructure of OPC-pellets, investigated through SEM analysis, was composed of soil minerals embedded within an amorphous matrix of cement hydration products (Fig. 4a, b). EDX analysis performed on different points of the cementitious matrix revealed the presence of Pb together with elements that are typical of cement phases (i.e., Ca, Si, Al and Mg). Elemental mapping showed that Pb was well dispersed within the matrix and was particularly concentrated on the surfaces of unhydrated cement particles (Fig. 4c, d). This Pb-rich layer on cement grains was also visible in back-scattered electron images as a white halo on light gray particles (Fig. 4e, f). Since the Kα emission line of S (2.30 eV) almost coincides with the Mα line of Pb (2.34 eV), the actual presence of Pb was determined thanks to its Lα line (10.5 eV). Experiments conducted by Ahn and coworkers (Ahn et al., 2015), who hydrated cement in the presence of $Pb(NO_3)_2$, showed the rapid formation of a gelatinous coating of lead nitrates and sulfates around cement particles, which had a protective effect that inhibited hydration. In our system after the dissolution of anglesite due to the high pH, Pb^{2+} ions may have formed such a coating on clinker particles, preventing and slowing the hydration reactions. The low hydration degree could also be related to the scarce availability of water for cement particles due to the presence of soil, which may have adsorbed part of the water otherwise available for cement hydration.

The 24 -h leaching test in ultrapure water (UNI 12457-4:2004) resulted in a Pb concentration in the eluate of 2040 ± 90 μg·L^{-1}, indicating retention of about 99.93% of the total Pb, with pH of 12.3. The results of the UNI 14429 leaching test performed at various pH values, ranging from 2.0 to 12.7, are reported in Fig. 5 and Table S12 for both the untreated soil and the OPC-pellets.

Pb behavior was highly pH-dependent, as expected based on its amphoteric nature, exhibiting lower mobilization at circum-neutral pH. In the case of the untreated soil, the minimum for Pb leaching (i.e., 0.01 mg L^{-1}) was reached at a pH of ca. 9, while between pH 7.0 and 4.5 Pb release was stable approximately at 0.2 mg L^{-1}. A clear increase was found for both pH lower than 4 and higher than 9, where the highest release from the contaminated soil was reached between pH 12 and 13. As observed in Fig. 5, the pelletization with OPC provided a reduction in Pb mobility within the pH range 10–13 by nearly an order of magnitude. Treatment with OPC also shifted the minimum solubility to a pH of 10. In both untreated soil and OPC-pellets, Pb release was enhanced at highly acid and alkaline pH levels. However, the ratio between its mobility in those extreme pH ranges was different in the two systems, as reported in the right-hand part of Fig. 5. While 8.6% of the total Pb was leached from untreated soil at pH 12.7, only 0.9% was

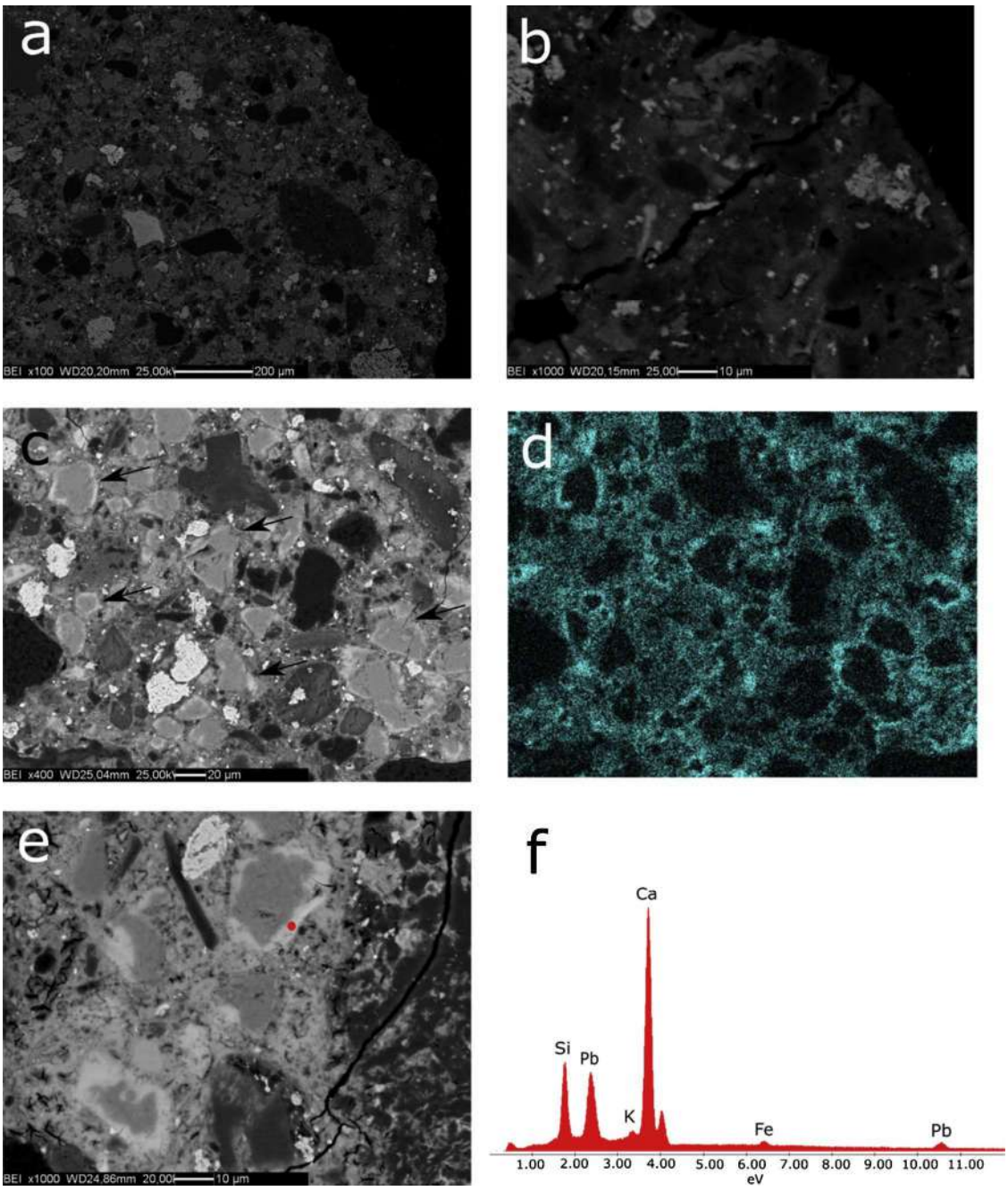

Fig. 4. SEM micrographs of polished sections of OPC-pellets. (a) Internal microstructure with soil particles embedded within the amorphous matrix given by cement; (b) soil particles dissolving in the alkaline medium; (c) internal microstructure showing unhydrated clinker particles (arrows); (d) map of Pb relative to image c obtained by choosing only the Pb signal at 10.5 eV to exclude S interferences; (e) high magnification image showing cement particles surrounded by a Pb-rich white halo; and (f) EDX spectrum correspondent to the red point in image (e). (For interpretation of the references to colour in this figure legend, the reader is referred to the web version of this article).

released from pellets in the same pH conditions. In an acidic environment, the situation was reversed: the percentage of leached Pb from OPC-pellets was higher with respect to untreated soil (2.5% versus 0.3% of the total Pb content, respectively). These differences indicate the stabilization of Pb within the S/S matrix, with a change in its geochemical speciation after treatment with OPC. As the stabilized material was maintained within a range of pH that is suitable for C-S-H phase stability (i.e., within 10 and 13), Pb was well-retained by the cementitious matrix, even if the pH was unsuitable for anglesite stabi- lity. This is because the metal underwent a change in its physical-che- mical form with cement constituents, in which anglesite was no longer stable. When pH dropped below 4, the greater sensitivity of the C-S-H phase to acidic conditions with respect to anglesite led to a greater leaching of Pb. These leaching tests can also be considered as a qualitative estimate of long-term leaching behavior of both materials. In fact various contaminated materials stabilized with OPC have been reported to shift towards less alkaline pH due to carbonation (Zhang et al., 2017b; Pandey et al., 2012), and soils subjected to acid mine drainage phenomena have been found to reach pH values lower than 3 (Liu et al., 2018). The results reported in Fig. 5 indicate that OPC-pellets have higher long-term environmental compatibility than untreated soil, because their Pb leaching decreases with the gradual lowering of pH, while the release of Pb from the untreated soil continues with progressing acidification due to acid mine drainage phenomena (Dong

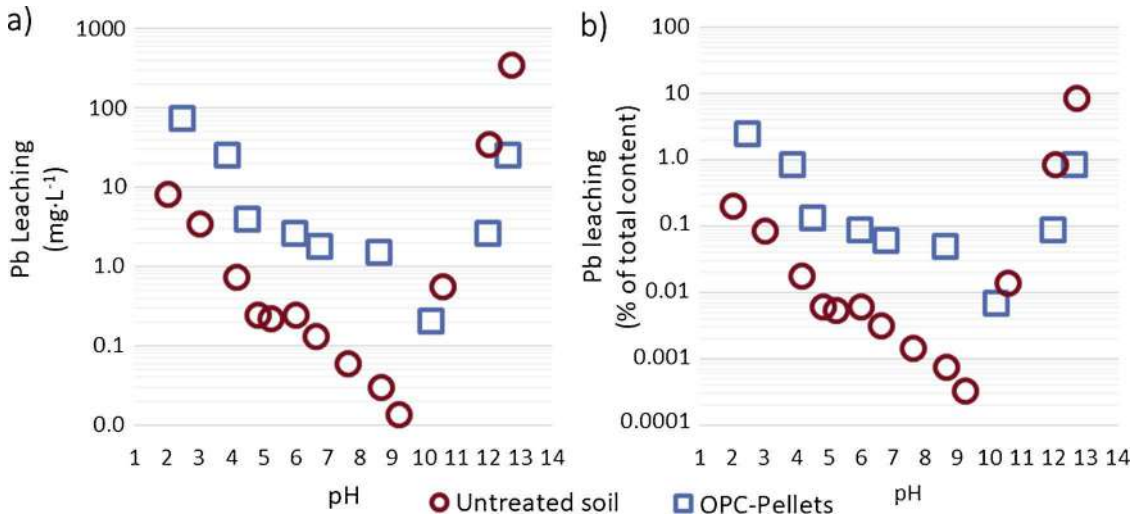

Fig. 5. Pb leaching as a function of pH – comparison of untreated soil and OPC-pellets. The release is expressed as mg·L^{-1} of Pb in the eluate (a) and as percentage of leached Pb with respect to total amount in the starting material (b).

et al., 2018; Kefeni et al., 2017).

3.4. Pelletization with CAC

XRD analysis of CAC-pellets is reported in Fig. 3a and Table S11. The amount of ettringite was doubled in comparison to that detected in the OPC-pellets. Ettringite does not usually form from the hydration of pure CAC because of the absence of sulfates. In CAC-soil system, calcium and aluminate ions derived from the dissolution of $CaAl_2O_4$ (CA) and $CaAl_4O_7$ (CA_2) reacted with the $(SO4)^{2-}$ ions present in the soil to produce ettringite. CAC promoted ettringite formation with respect to OPC as it supplied more aluminate ions, which were the limiting factor for its formation in the OPC system. Other CAC hydration phases found were gibbsite ($Al(OH)_3$), hydrogarnet ($Ca_3[Al(OH)_6]_2$) and a metastable calcium aluminum hydrate ($CaAl_2[OH]_8[H_2O]_{5.4}$). As expected, the amount of amorphous fraction was lower with respect to OPC-pellets, as the C-S-H phase typically is not a product of CAC hydration. Unhydrated CAC phases (~40% of the total cement) were quantified in an amount comparable to that observed in the OPC system, indicating the same degree of hydration's reduction. SEM analysis showed, as in the case of OPC-pellets, that the internal microstructure was composed of soil minerals and clinker particles surrounded by an amorphous matrix (Fig. 6a). The cracks observed throughout the analyzed areas (Fig. 6b) could be attributed to the high vacuum condition reached during the analysis, which promoted the dehydration of ettringite with subsequent shrinkage and cracking of the cement matrix. This phenomenon, which is known in the literature (Thiéry et al., 2017), was also ascertained by conducting an additional investigation with an environmental scanning electron microscope (ESEM) not reported in this paper. EDX analysis also confirmed the existence of ettringite in correspondence to areas with intense cracking.

Elemental mapping of lead and sulfur relatively to Fig. 6b is reported in Fig. 6c and d. Pb appeared associated with S in the cracked regions of ettringite. A detailed investigation of the cracked domains with a FESEM equipped with WDS (Fig. 6e) indicated a chemical composition compatible to ettringite with a certain degree of substitution of Pb^{2+} for Ca^{2+} (Gougar et al., 1996). Contrary to the OPC-pellets, where Pb formed a coating on clinker particles, in CAC-pellets no Pb-enrichment was observed on CA and CA_2 clinker phases. A delayed hydration in CAC doped with $Pb(NO_3)_2$ was observed in recent studies (Navarro-Blasco et al., 2013; Duran et al., 2016), but the mechanisms involved are still not completely understood. The results of the leaching test in ultrapure water revealed a Pb concentration of 73.2 ± 9.4 μg·L^{-1}, meaning an almost complete retention of Pb, consistently with results reported in the literature (Voglar and Leštan, 2013; Navarro-Blasco et al., 2013; Okoronkwo et al., 2018; Fernández et al., 2014). The pH of CAC-pellets was slightly lower compared to OPC-pellets (12.0 vs 12.3, respectively, as measured after the 24 -h leaching test) indicating a more favorable condition for Pb immobilization. However, the small difference in pH values hardly explains the significant lowering of Pb leaching after treatment with CAC. We hypothesized that the increased and rapid precipitation of ettringite has promoted the sequestration of Pb ions from the pore solution in the early phases of hydration. XRD analysis, coupled with the results of the leaching test clearly attest that ettringite represents the low-solubility species that trapped Pb, as confirmed by WDS data indicating that Pb is associated with ettringite structural elements. For these reasons, our proposed interpretation involves both physical encapsulation and chemical fixation as mechanisms involved in Pb immobilization after treatment with CAC in the presence of sulfates. Despite various studies reporting the influence of pH, temperature, soluble components and dissolved CO_2 on ettringite stability (Shi et al., 2016; Wang et al., 2016a; Balonis, 2019; Plank et al., 2016), these data are not enough to fully predict ettringite durability in this case study, since substituted ettringite showed different behavior compared to the unsubstituted form (Guo et al., 2017c; Wieczorek-Ciurowa et al., 2001; Palou et al., 2009; Wang et al., 2017). In light of this we are aware that investigations on Pb-substituted ettringite stability are needed.

3.5. Pelletization with metakaolin

The treatment of the contaminated soil with NaOH-activated metakaolin produced pellets with the composition reported in Fig. 3b and Table S11. Given the amorphous nature of both metakaolin and the derived geopolymeric gel, the phase assemblage was difficult to characterize with XRD analysis alone. The only new crystalline phases formed in MK-pellets were thenardite (Na_2SO_4), mirabilite ($Na_2SO_4{\cdot}10H_2O$) and burkeite ($Na_6(CO_3)(SO_4)_2$), which were derived from the interaction between sulfates from the soil and NaOH. These pellets presented an internal microstructure characterized by high porosity and a less-dense structure (Fig. 7a), which caused a very low mechanical resistance. This could be ascribed to both highly hygroscopic salts (thenardite) leading to expansion phenomena (Lopez-Arce and Doehne, 2006) and to a limited dissolution of metakaolin due to relatively low molarity of the activating solution (4 M NaOH). In addition, the lack of readily available silica may have also impeded the formation of a well-developed geopolymeric gel (Valentini, 2018).

An in depth investigation of the microstructure revealed the

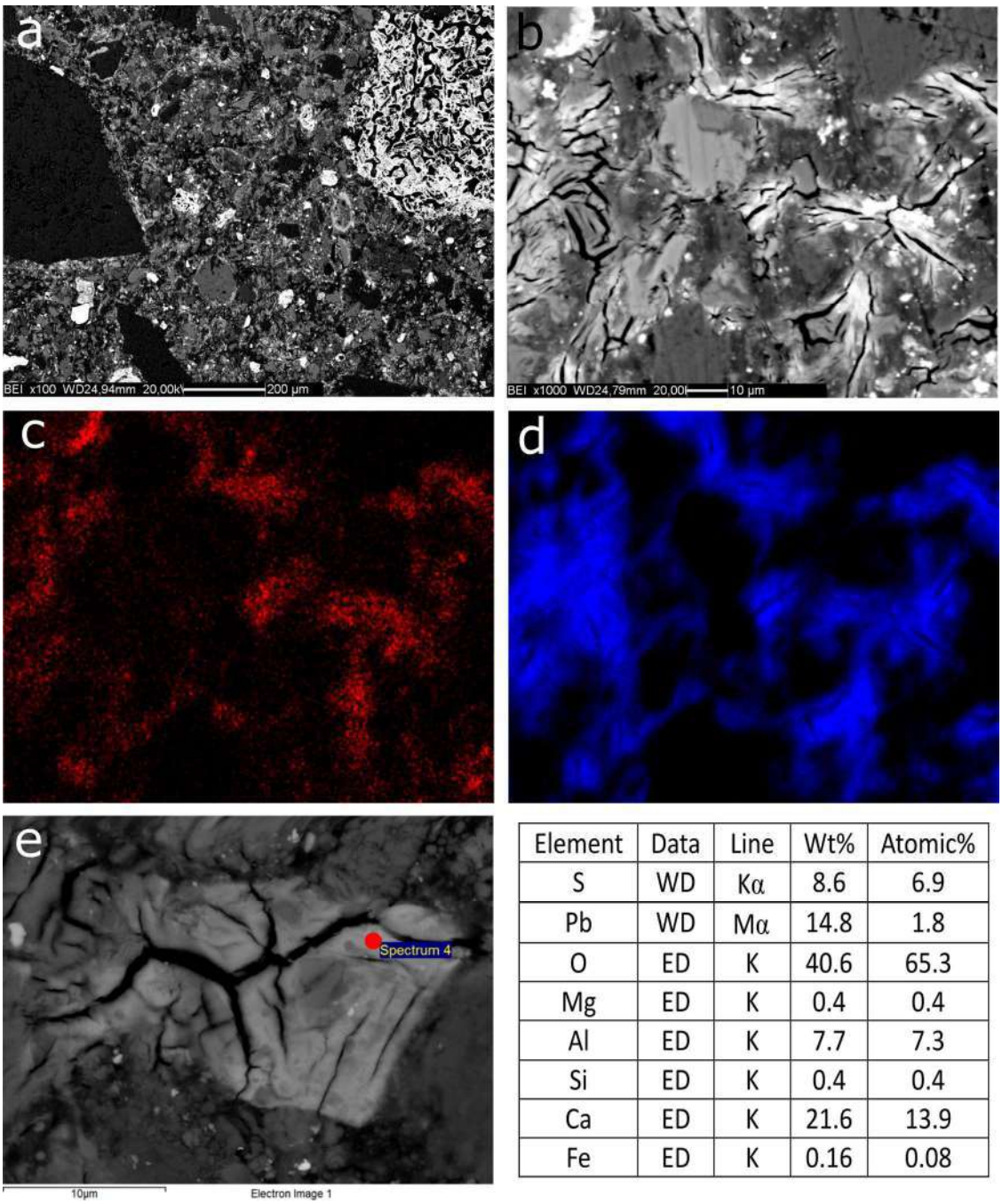

Element	Data	Line	Wt%	Atomic%
S	WD	Kα	8.6	6.9
Pb	WD	Mα	14.8	1.8
O	ED	K	40.6	65.3
Mg	ED	K	0.4	0.4
Al	ED	K	7.7	7.3
Si	ED	K	0.4	0.4
Ca	ED	K	21.6	13.9
Fe	ED	K	0.16	0.08

Fig. 6. SEM micrographs of polished sections of CAC-pellets. (a) Internal microstructure; (b) Internal microstructure at higher magnification showing the cracks for the dehydration of ettringite in the high vacuum conditions; (c) map of Pb relative to image (b); (d) map of S relative to image (b); (e) FESEM image of ettringite with the chemical composition of the red point reported (WD = wavelength dispersive, ED = energy dispersive). (For interpretation of the references to colour in this figure legend, the reader is referred to the web version of this article).

presence of Pb inside some aggregates with dimensions of ca. 100–200 µm (Fig. 7b) that were composed of clusters of soil minerals (grey particles in Fig. 7b) surrounded by an amorphous Pb-rich gel-like phase, white-colored at back-scattered electron detection (Fig. 7c). Despite the loosely bound structure, the results of leaching test showed a concentration of Pb in the eluate of 194 ± 10 µg·L^{-1}, signifying the almost total retention of this contaminant. This result demonstrates how the eluate pH (10.4, as measured at the end of the 24 h leaching test) played a fundamental role in the retention of this heavy metal (Lewis, 2010; Wang et al., 2016b), despite the high surface area exposed to leaching due to the pellets low mechanical resistance. We hypothesize that an amorphous phase with a high Pb concentration may also have contributed, together with the mild alkaline pH of the eluate, to the low release observed from the MK-pellets. Given the amorphous character of the geopolymeric binder, XRD data were of limited utility in elucidating the mechanism implied in Pb retention. Further work on MK systems is required for a better comprehension of this promising binder in S/S applications.

4. Conclusions

In this study the use of three different binders (OPC, CAC, MK) for the solidification/stabilization of Pb were investigated, showing how the various hydration products provided different immobilization

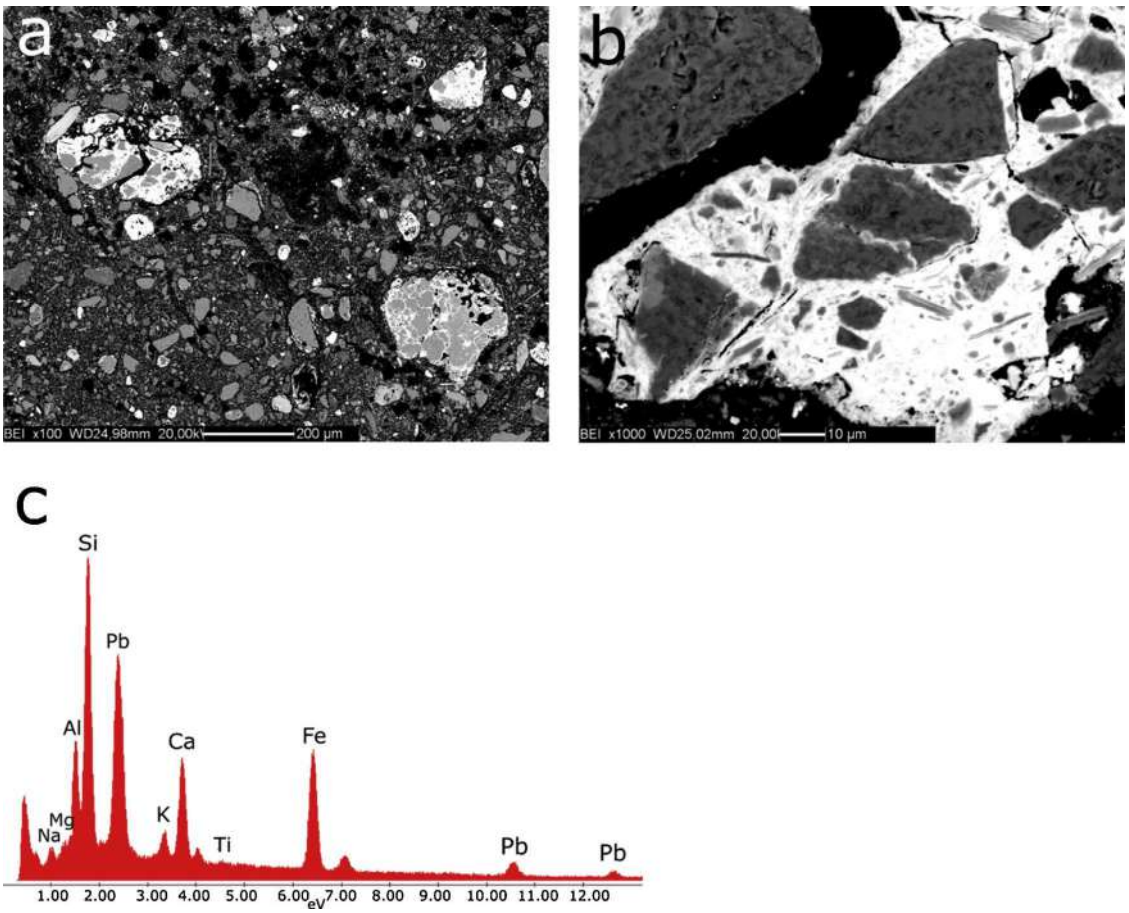

Fig. 7. SEM micrographs of the polished sections of MK-pellets. (a) Internal microstructure showing high porosity and light gray/white aggregates; (b) aggregate composed of soil phases (gray) embedded in a matrix (white); and (c) elemental composition of the white-colored phase in image (b).

mechanisms and performances. With OPC the C-S-H formation could host Pb ions likely adsorbed on its surface. The analysis of this system at different pH permitted to indicate an optimal pH for Pb retention, which revealed to be close to 10. The pH of a carbonated cementitious material decreases with respect to the initial pH values, suggesting that the Pb-retention in OPC-pellets can increase in the long term. In the case of CAC binder, the high concentration of sulfates in the soil drastically shifted the reactivity toward ettringite formation, where Pb^{2+} was found replacing part of calcium in the crystalline structure. The lowering of Pb mobilization in CAC system and SEM-WDS analyses indicated that ettringite had a leading role in the retention of this contaminant. NaOH-activated metakaolin was studied for exploring the use of geopolymers in S/S applications, including only one precursor (MK) and one alkaline activator (NaOH solution) to limit the number of variables involved. The high retention of Pb in MK-pellets was partly related to the relatively low pH of the system and we also hypothesize the role of an amorphous phase contributing with chemical fixation. Despite the promising results of the leaching test with regard to Pb, we are aware that future research is needed to overcome the lack of solidification. Additionally, the use of a different alkaline solution for metakaolin activation could be a way to avoid the formation of unwanted Na salts. As far as the other heavy metals present in the contaminated soil, further work is in progress to assess the performance of the discussed binders for their immobilization.

References

Enviromental Ministry Decree EMD, 2006. Legislative Decree n°152 of 03rd April 2006. Italian Official Gazzette N. 88 of 14th April 2006.

Aguilar-Carrillo, J., Herrera, L., Gutiérrez, E.J., Reyes-Domínguez, I.A., 2018. Solid-phase distribution and mobility of thallium in mining-metallurgical residues: environmental hazard implications. Environ. Pollut. 243, 1833–1845. https://doi.org/10.1016/j.envpol.2018.10.014.

Ahn, T.H., Shim, K.B., So, K.H., Ryou, J.S., 2014. Influence of lead and chromium ions as toxic heavy metals between AFt and AFm phases based on C3A and C4A3S. J. Ceram. Process. Res. 15, 539–544. (Accessed July 13, 2019). http://jcpr.kbs-lab.co.kr/file/JCPR_vol.15_2014/JCPR15-6/_322014-064_539-544.pdf.

Ahn, T.-H., Shim, K.-B., Sho, K.-H., 2015. Influence of lead, chromium and zinc ions as toxic heavy metals between C-S-H phases based on C3S. J. Ceram. Process. Res. 40–44. (Accessed July 12, 2019). https://pdfs.semanticscholar.org/af72/2fef86441243043a838752c43ee65e2b5127.pdf.

Akcil, A., Koldas, S., 2006. Acid Mine Drainage (AMD): causes, treatment and case studies. J. Clean. Prod. 14, 1139–1145. https://doi.org/10.1016/j.jclepro.2004.09.006.

Arnold, M.C., de Vargas, A.S., Bianchini, L., 2017. Study of electric-arc furnace dust (EAFD) in fly ash and rice husk ash-based geopolymers. Adv. Powder Technol. 28, 2023–2034. https://doi.org/10.1016/j.apt.2017.05.007.

Bakhshi, N., Sarrafi, A., Ramezanianpour, A.A., 2019. Immobilization of hexavalent chromium in cement mortar: leaching properties and microstructures. Environ. Sci. Pollut. Res. 26, 20829–20838. https://doi.org/10.1007/s11356-019-05301-z.

Balonis, M., 2019. Thermodynamic modelling of temperature effects on the mineralogy of

Portland cement systems containing chloride. Cem. Concr. Res. 120, 66–76. https://doi.org/10.1016/j.cemconres.2019.03.011.
Batchelor, B., 2006. Overview of waste stabilization with cement. Waste Manag. 26, 689–698. https://doi.org/10.1016/j.wasman.2006.01.020.
Bettiol, C., Stievano, L., Bertelle, M., Delfino, F., Argese, E., 2008. Evaluation of microwave-assisted acid extraction procedures for the determination of metal content and potential bioavailability in sediments. Appl. Geochem. 23, 1140–1151. https://doi.org/10.1016/j.apgeochem.2007.11.008.
Bigham, J.M., Nordstrom, D.K., 2011. Iron and aluminum hydroxysulfates from acid sulfate waters. Rev. Mineral. Geochem. 40, 351–403. https://doi.org/10.2138/rmg.2000.40.7.
Bonomo, L., Careghini, A., Dastoli, S., De Propris, L., Ferrari, G., Gabellini, M., Saponaro, S., 2009. Feasibility studies for the treatment and reuse of contaminated marine sediments. Environ. Technol. 30, 817–823. https://doi.org/10.1080/09593330902990105.
Bougharraf, N., Louati, D., Mosbahi, M., Rouis, M.J., Rigane, H., 2018. Comparison of the effectiveness of different binders in solidification/stabilization of a contaminated soil. Arab. J. Geosci. 11, 348. https://doi.org/10.1007/s12517-018-3668-2.
British Standards Institution, 2005. Tests for geometrical properties of aggregates Part 1: Determination of Particle Size Distribution - Sieving Method. Bs En 933–11997 (3), 1–7. https://doi.org/10.1186/cc9013.
British Standards Institution, 2004. Characterisation of Waste - Leaching - Compliance Test for Leaching of Granular Waste Materials and Sludges - Part 4: One Stage Batch Test at a Liquid to Solid Ratio of 10 l/kg for Materials With Particle Size Below 10 Mm (without or With Size Reduction).
British Standards Institution, 2015. Characterization of Waste — Leaching Behaviour Test — Influence of pH on Leaching With Initial Acid / Base Addition.
Chen, Q.Y., Tyrer, M., Hills, C.D., Yang, X.M., Carey, P., 2009. Immobilisation of heavy metal in cement-based solidification/stabilisation: a review. Waste Manag. 29, 390–403. (Accessed November 19, 2018). https://www.sciencedirect.com/science/article/pii/S0956053X08000548.
Daniil, A., Dimitrakopulos, G.P., Varitis, S., Vourlias, G., Kaimakamis, G., Pantazopoulou, E., Pavlidou, E., Zouboulis, A.I., Karakostas, T., Komninou, P., 2018. Stabilization of Cr-rich tannery waste in fly ash matrices. Waste Manag. Res. 36, 818–826. https://doi.org/10.1177/0734242X18775488.
Dong, Y., Liu, F., Qiao, X., Zhou, L., Bi, W., 2018. Effects of acid mine drainage on calcareous soil characteristics and Lolium perenne L. Germination. Int. J. Environ. Res. Public Health 15, 2742. https://doi.org/10.3390/ijerph15122742.
Dove, P.M., Czank, C.A., 1995. Crystal chemical controls on the dissolution kinetics of the isostructural sulfates: celestite, anglesite, and barite. Geochim. Cosmochim. Acta 59, 1907–1915. https://doi.org/10.1016/0016-7037(95)00116-6.
Duran, A., Sirera, R., Pérez-Nicolás, M., Navarro-Blasco, I., Fernández, J.M.M., Alvarez, J.I.I., 2016. Study of the early hydration of calcium aluminates in the presence of different metallic salts. Cem. Concr. Res. 81, 1–15. https://doi.org/10.1016/j.cemconres.2015.11.013.
Falzone, G., Balonis, M., Sant, G., 2015. X-AFm stabilization as a mechanism of bypassing conversion phenomena in calcium aluminate cements. Cem. Concr. Res. 72, 54–68. https://doi.org/10.1016/j.cemconres.2015.02.022.
Fansuri, H., Subaer, W., Supriadi, D., Hartanto, N., Widiastuti, 2019. The kinetics of Cd 2+ and Pb 2+ leaching from fly ash geopolymers. Chem. Eng. Trans. 72. https://doi.org/10.3303/CET1972040.
Fernández, J.M., Navarro-Blasco, I., Duran, A., Sirera, R., Alvarez, J.I., 2014. Treatment of toxic metal aqueous solutions: encapsulation in a phosphate-calcium aluminate matrix. J. Environ. Manage. 140, 1–13. https://doi.org/10.1016/j.jenvman.2014.01.044.
Fernández-Pereira, C., Luna-Galiano, Y., Pérez-Clemente, M., Leiva, C., Arroyo, F., Villegas, R., Vilches, L.F., 2018. Immobilization of heavy metals (Cd, Ni or Pb) using aluminate geopolymers. Mater. Lett. 227, 184–186. https://doi.org/10.1016/j.matlet.2018.05.027.
Ferrari, G., Artioli, G., Parisatto, M., 2010. From HPC to HPSS: The Use Of Superplasticizers For The Improvement of S/S Technology. S/S Tech - Int. Solidif. Forum, pp. 193–203.
Gougar, M.L.D.D., Scheetz, B.E., Roy, D.M., 1996. Ettringite and C-S-H portland cement phases for waste ion immobilization: a review. Waste Manag. 16, 295–303. https://doi.org/10.1016/S0956-053X(96)00072-4.
Guo, B., Liu, B., Yang, J., Zhang, S., 2017a. The Mechanisms of Heavy Metal Immobilization by Cementitious Material Treatments and Thermal Treatments: A Review. Academic Presshttps://doi.org/10.1016/j.jenvman.2017.02.026.
Guo, B., Pan, D., Liu, B., Volinsky, A.A., Fincan, M., Du, J., Zhang, S., 2017b. Immobilization mechanism of Pb in fly ash-based geopolymer. Constr. Build. Mater. 134, 123–130. https://doi.org/10.1016/j.conbuildmat.2016.12.139.
Guo, B., Sasaki, K., Hirajima, T., 2017c. Characterization of the intermediate in formation of selenate-substituted ettringite. Cem. Concr. Res. 99, 30–37. https://doi.org/10.1016/j.cemconres.2017.05.002.
He, H., Suito, H., 2008. Immobilization of hexavalent chromium in aqueous solution through the formation of 3CaO (Al,Fe)2O3 Ca(OH)2 xH2O phase, ettringite and C-S-H gel. ISIJ Int. 42, 139–145. https://doi.org/10.2355/isijinternational.42.139.
Ivanov, R.C., Angulski da Luz, C., Zorel, H.E., Pereira Filho, J.I., 2016. Behavior of calcium aluminate cement (CAC) in the presence of hexavalent chromium. Cem. Concr. Compos. 73, 114–122. https://doi.org/10.1016/j.cemconcomp.2016.07.006.
Joussein, E., Soubrand, M., Pascaud, G., Cogulet, A., Rossignol, S., 2019. Immobilization of Pb from mine sediments in metakaolin-based geomaterials. Environ. Sci. Pollut. Res. 26, 14473–14482. https://doi.org/10.1007/s11356-019-04737-7.
Kefeni, K.K., Msagati, T.A.M., Mamba, B.B., 2017. Acid mine drainage: prevention, treatment options, and resource recovery: a review. J. Clean. Prod. 151, 475–493. https://doi.org/10.1016/j.jclepro.2017.03.082.
Koplík, J., Pořízka, J., Kalina, L., Másilko, J., Březina, M., 2018. Influence of Pb dosage on immobilization characteristics of different types of alkali-activated mixtures and mortars. Adv. Mater. Sci. Eng. Int. J. 2018, 1–6. https://doi.org/10.1155/2018/4026127.
Krauskopf, K.B., 1956. Dissolution and precipitation of silica at low temperatures. Geochim. Cosmochim. Acta 10, 1–26. https://doi.org/10.1016/0016-7037(56)90009-6.
Łach, M., Mierzwiński, D., Korniejenko, K., Mikuła, J., Hebda, M., 2018. Geopolymers as a material suitable for immobilization of fly ash from municipal waste incineration plants. J. Air Waste Manag. Assoc. 68, 1190–1197. https://doi.org/10.1080/10962247.2018.1488772.
Lea, F.M., 2004. Lea's Chemistry of Cement and Concrete, fourth edi. Elsevierhttps://doi.org/10.1016/B978-0-7506-6256-7.50031-X.
Lewis, A.E., 2010. Review of metal sulphide precipitation. Hydrometallurgy 104,222–234. https://doi.org/10.1016/j.hydromet.2010.06.010.
Li, Y., Min, X., Ke, Y., Fei, J., Liu, D., Tang, C., 2019. Immobilization potential and immobilization mechanism of arsenic in cemented paste backfill. Miner. Eng. 138, 101–107. https://doi.org/10.1016/j.mineng.2019.04.041.
Li, X., He, C., Bai, Y., Ma, B., Wang, G., Tan, H., 2014. Stabilization/solidification on chromium (III) wastes by C3A and C3A hydrated matrix. J. Hazard. Mater. 268, 61–67. https://doi.org/10.1016/j.jhazmat.2014.01.002.
Liu, F., Qiao, X., Zhou, L., Zhang, J., 2018. Migration and fate of acid mine drainage pollutants in calcareous soil. Int. J. Environ. Res. Public Health 15, 1759. https://doi.org/10.3390/ijerph15081759.
Lopez-Arce, P., Doehne, E., 2006. Kinetics of sodium sulfate efflorescence as observed by humidity cycling with ESEM. Heritage, Weather. Conserv. Conf.
Lu, L., He, Y., Xiang, C., Wang, F., Hu, S., 2019. Distribution of heavy metal elements in chromium (III), lead-doped cement pastes. Adv. Cem. Res. 31, 270–278. https://doi.org/10.1680/jadcr.17.00114.
Lv, Y., Li, X., De Schutter, G., Ma, B., 2016. Stabilization of Cr(III) wastes by C3S and C3S hydrated matrix: comparison of two incorporation methods. Mater. Struct. Constr. 49, 3109–3118. https://doi.org/10.1617/s11527-015-0707-2.
Mao, Y., Muhammad, F., Yu, L., Xia, M., Huang, X., Jiao, B., Shiau, Y., Li, D., 2019. The solidification of lead-zinc smelting slag through bentonite supported alkali-activated slag cementitious material. Int. J. Environ. Res. Public Health 16, 1121. https://doi.org/10.3390/ijerph16071121.
Mulligan, C.N., Yong, R.N., Gibbs, B.F., 2001. Remediation technologies for metal-contaminated soils and groundwater: an evaluation. Eng. Geol. 60, 193–207. https://doi.org/10.1016/S0013-7952(00)00101-0.
Navarro-Blasco, I., Duran, A., Sirera, R., Fernández, J.M., Alvarez, J.I., 2013. Solidification/stabilization of toxic metals in calcium aluminate cement matrices. J. Hazard. Mater. 260, 89–103. https://doi.org/10.1016/J.JHAZMAT.2013.04.048.
Nematollahi, B., Sanjayan, J., 2014. Efficacy of available superplasticizers on geopolymers. Res. J. Appl. Sci. Eng. Technol. 7, 1278–1282. https://doi.org/10.19026/rjaset.7.420.
Niu, M., Li, G., Wang, Y., Li, Q., Han, L., Song, Z., 2018. Comparative study of immobilization and mechanical properties of sulfoaluminate cement and ordinary Portland cement with different heavy metals. Constr. Build. Mater. 193, 332–343. https://doi.org/10.1016/j.conbuildmat.2018.10.206.
Okoronkwo, M.U., Balonis, M., Katz, L., Juenger, M., Sant, G., 2018. A thermodynamics-based approach for examining the suitability of cementitious formulations for solidifying and stabilizing coal-combustion wastes. J. Environ. Manage. 217, 278–287. https://doi.org/10.1016/j.jenvman.2018.02.095.
Palou, M., Majling, J., Drábik, M., Ayadi, A., 2009. Ettringite & its Chromate Analogue, Structure and Thermal Stability. Solid State Phenom. 90–91, 395–400. https://doi.org/10.4028/www.scientific.net/ssp.90-91.395.
Pandey, B., Kinrade, S.D., Catalan, L.J.J., 2012. Effects of carbonation on the leachability and compressive strength of cement-solidified and geopolymer-solidified synthetic metal wastes. J. Environ. Manage. 101, 59–67. https://doi.org/10.1016/j.jenvman.2012.01.029.
Plank, J., Zhang-Preße, M., Ivleva, N.P., Niessner, R., 2016. Stability of single phase C3A hydrates against pressurized CO2. Constr. Build. Mater. 122, 426–434. https://doi.org/10.1016/j.conbuildmat.2016.06.042.
Scanferla, P., Ferrari, G., Pellay, R., Volpi Ghirardini, A., Zanetto, G., Libralato, G., Pellay, R., Volpi Ghirardini, A., Zanetto, G., Libralato, G., Pellay, R., Volpi Ghirardini, A., Zanetto, G., Libralato, G., 2009. An innovative stabilization/solidification treatment for contaminated soil remediation: demonstration project results. J. Soils Sediments 9, 229–236. https://doi.org/10.1007/s11368-009-0067-z.
Shi, C., Fernández-Jiménez, A., 2006. Stabilization/solidification of hazardous and radioactive wastes with alkali-activated cements. J. Hazard. Mater. 137, 1656–1663.
Shi, C., Zhang, G., He, T., Li, Y., 2016. Effects of superplasticizers on the stability and morphology of ettringite. Constr. Build. Mater. 112, 261–266. https://doi.org/10.1016/j.conbuildmat.2016.02.198.
Stoffregen, R.E., Alpers, C.N., Jambor, J.L., 2011. Alunite-jarosite crystallography, thermodynamics, and geochronology. Rev. Mineral. Geochem. 40, 453–479. https://doi.org/10.2138/rmg.2000.40.9.
Su, Y., Yang, J., Liu, D., Zhen, S., Lin, N., Zhou, Y., 2016. Solidification/stabilization of simulated cadmium-contaminated wastes with magnesium potassium phosphate cement. Int. J. Civ. Struct. Environ. Infrastruct. Eng. Res. Dev. 21, 15–21. https://doi.org/10.4491/eer.2015.092.
Taylor, H.F.W., 2003. Cement chemistry. Cem. Concr. Compos. 20, 335. https://doi.org/10.1016/s0958-9465(98)00023-7.
Thiéry, V., Trincal, V., Davy, C.A., 2017. The elusive ettringite under the high-vacuum SEM – a reflection based on natural samples, the use of Monte Carlo modelling of EDS analyses and an extension to the ettringite group minerals. J. Microsc. 268, 84–93. https://doi.org/10.1111/jmi.12589.

Valentini, L., 2018. Modeling dissolution–Precipitation kinetics of alkali-activated metakaolin. ACS Omega 3, 18100–18108. https://doi.org/10.1021/acsomega.8b02380.
van Jaarsveld, J.G.S., van Deventer, J.S.J., Lorenzen, L., 1997. Potential use of geopolymeric materials to immobilize toXic metals: part I. Theory and applications. Miner. Eng. 10, 659–669. https://doi.org/10.1016/S0892-6875(97)00046-0.
Voglar, G.E., Leštan, D., 2013. Equilibrium leaching of toXic elements from cement stabilized soil. J. Hazard. Mater. 246–247, 18–25. https://doi.org/10.1016/j.jhazmat.2012.11.058.
Vollpracht, A., Brameshuber, W., 2016. Binding and leaching of trace elements in Portland cement pastes. Cem. Concr. Res. 79, 76–92. https://doi.org/10.1016/j.cemconres.2015.08.002.
Wang, Z., Guo, C., Song, Y., Wang, B., Xu, H., 2016a. Stability of thaumasite and ettringite. Kuei Suan Jen Hsueh Pao/J. Chin. Ceram. Soc. 44, 292–298. https://doi.org/10.14062/j.issn.0454-5648.2016.02.16.
Wang, P., Xue, Q., Li, J.-S., Zhang, T.-T., 2016b. Effects of pH on leaching behavior of compacted cement solidified/stabilized lead contaminated soil. Environ. Prog. Sustain. Energy 35, 149–155. https://doi.org/10.1002/ep.12218.
Wang, W., Shao, Y., Hou, H., Zhou, M., 2017. Synthesis and thermodynamic properties of arsenate and sulfate-arsenate ettringite structure phases. PLoS One 12, e0182160. https://doi.org/10.1371/journal.pone.0182160.
Wang, Y.S., Dai, J.G., Wang, L., Tsang, D.C.W., Poon, C.S., 2018a. Influence of lead on stabilization/solidification by ordinary Portland cement and magnesium phosphate cement. Chemosphere. 190, 90–96. https://doi.org/10.1016/j.chemosphere.2017.09.114.
Wang, L., Yu, K., Li, J.S., Tsang, D.C.W., Poon, C.S., Yoo, J.C., Baek, K., Ding, S., Hou, D., Dai, J.G., 2018b. Low-carbon and low-alkalinity stabilization/solidification of high-Pb contaminated soil. Chem. Eng. J. 351, 418–427. https://doi.org/10.1016/j.cej.2018.06.118.
Wang, L., Cho, D.W., Tsang, D.C.W., Cao, X., Hou, D., Shen, Z., Alessi, D.S., Ok, Y.S., Poon, C.S., 2019. Green remediation of As and Pb contaminated soil using cement-free clay-based stabilization/solidification. Environ. Int. 126, 336–345. https://doi.org/10.1016/j.envint.2019.02.057.
Wieczorek-Ciurowa, K., Fela, K., Kozak, A.J., 2001. Chromium(III)-ettringite formation and its thermal stability. in: J. Therm. Anal. Calorim 655–660. https://doi.org/10.1023/A:1017978414203.
Yang, C., Chen, Y., Peng, P., Li, C., Chang, X., Wu, Y., 2009. Trace element transformations and partitioning during the roasting of pyrite ores in the sulfuric acid industry. J. Hazard. Mater. 167, 835–845. https://doi.org/10.1016/j.jhazmat.2009.01.067.
Zhang, M., Yang, C., Zhao, M., Yu, L., Yang, K., Zhu, X., Jiang, X., 2018. Immobilization of Cr(VI) by hydrated Portland cement pastes with and without calcium sulfate. J. Hazard. Mater. 342, 242–251. https://doi.org/10.1016/j.jhazmat.2017.07.039.
Zhang, Y., Zhang, S., Ni, W., Yan, Q., Gao, W., Li, Y., 2019. Immobilisation of high-arsenic-containing tailings by using metallurgical slag-cementing materials. Chemosphere 223, 117–123. https://doi.org/10.1016/j.chemosphere.2019.02.030.
Zhang, M., Yang, C., Zhao, M., Yang, K., Shen, R., Zheng, Y., 2017a. Immobilization potential of Cr(VI) in sodium hydroXide activated slag pastes. J. Hazard. Mater. 321, 281–289. https://doi.org/10.1016/j.jhazmat.2016.09.019.
Zhang, D., Cao, Z., Zhang, T., Su, X., 2017b. Effect of carbonation on leaching behavior, engineering properties and microstructure of cement-stabilized lead-contaminated soils. Environ. Earth Sci. 76, 724. https://doi.org/10.1007/s12665-017-7071-1.